University of Exeter coursework header sheet

ECMM102 Group Project (Meng) (A, TRM1+2 2014/5)

028836

1015549

610031603

Coursework: I2

Submission Deadline: Thu 30th Apr 2015 12:00

Personal tutor: Professor Philippe Young

Marker name: Gavin Tabor

Word count: 10977

By submitting coursework you declare that you understand and consent to the University policies regarding plagiarism and mitigation (these can be seen online at www.exeter.ac.uk/plagiarism, and www.exeter.ac.uk/mitigation respectively), and that you have read your school's rules for submission of written coursework, for example rules on maximum and minimum number of words. Indicative/first marks are provisional only.

First marker's comments

Indicative mark

Second marker's comments

Second mark

Moderator's comments

Agreed mark

I2 Report

Modelling of Turbulent Effects on a Bridge Deck Structure

Joseph Morgan

2015

4th year MEng Group Project

I certify that all material in this thesis that is not my own work has been identified and that no material has been included for which a degree has previously been conferred on me.

Signed.....

College of Engineering, Mathematics, and Physical Sciences
University of Exeter

I2 Report

ECMM102

Title: Modelling of Turbulent Effects on a Bridge Deck Structure
Word count: 10977
Number of pages: 40

Date of submission: Thursday, 30 April 2015

Student Name: Joseph Morgan
Programme: Mechanical Engineering (MEng)
Student number: 610031603
Candidate number: 028836

Supervisor: Dr. Gavin Tabor

Abstract

As engineers it is important that wind induced vibrations are properly understood and accounted for. Long span bridges are particularly susceptible to these vibrations. With computational power increasing, computational fluid dynamics (CFD) is becoming an increasingly viable option for modelling air flow. In this report the different types of wind induced vibrations are investigated, with particular interest in vortex shedding. Different turbulence models are investigated and it was determined that delayed detached eddy simulation (DDES) would be the most appropriate model for simulating turbulent flow over a bridge deck. A DDES simulation of airflow traveling at $1ms^{-1}$ across the Humber Bridge was simulated. The most common type of vortex shedding, the Von Kármán vortex street was shown to be suppressed by the geometry of the Humber Bridge. Single shear layer vortices were formed at the leading edge and did impart a small oscillating force on the bridge. The forces imparted on the bridge were recorded. Fast Fourier transfer analysis was carried out on the force data. The resulting frequencies produced by this analysis have been passed on to the structural subgroup for comparison purposes.

Keywords: Humber Bridge, delayed detached eddy simulation, vortex shedding, wind induced vibrations.

Table of contents

1. Introduction and background

With advances in technology and improvements to our understanding of engineering, modern bridges are being constructed larger and more efficiently than before. This has left bridges increasingly susceptible to different types of vibrational damage [1]. The possible causes of vibrational damage can be human motion, seismic activity, heavy traffic conditions or wind loading. The most well-known case of a bridge failing due to wind loading is the Tacoma Narrows Bridge. The suspension bridge which was constructed in 1938 started showing very large torsional oscillations at moderate wind speeds. In 1940 the bridge eventually collapsed in 40mph winds. The cause of the failure was deemed to be Aeroelastic flutter, caused by the positive feedback between the oscillating bridge and constant wind loading [2].

Disasters such as this one are unlikely to occur in modern bridges as they either tend to be over engineered, or are highly monitored, so that issues are detected early and can be resolved. The London Millennium Footbridge is an example of this. After the bridge opened, designers noticed that there were horizontal oscillations when large numbers of people walked over it. It was determined that the natural sway of the people walking caused a slight periodic motion in the bridge. This motion caused people to walk in step with each other, which in turn amplified the effects of the bridges swaying [3]. Fortunately the bridges designers were able to temporarily shut the bridge and install several dampers to prevent this effect from being so prevalent [3]. Unfortunately the closure of the bridge and subsequent installation of dampers will have cost a lot of money. Ideally these circumstances should be predicted before construction so that additional costs can be avoided.

With computing power steadily increasing, it is becoming cheaper and more viable to use computational fluid dynamics (CFD) to predict the effects that wind loading has on bridges. As this report will demonstrate, wind loading can cause continuous and potentially harmful vibrations throughout a bridges lifespan. As engineers, it is important that these vibrations are fully understood and accounted for.

1.1. Group Aims & Individual Aims

This group project aims to investigate the effects that wind loading has on a bridge deck, with particular interest in wind induced vibrations. For this project the Humber Bridge in Hull has been used as a case study. The project has been split into two subgroups.

1. ***The structural subgroup -*** is investigating the vibrational modes of Humber Bridge and the effects that they have.
2. ***The CFD subgroup -*** aims to create an accurate CFD model of turbulence over the Humber Bridge.

At the end of the project the two groups will come together to determine if a particular wind speed will cause the Humber Bridge to vibrate at one of its modes.

The creation of the CFD model has been split into three sections.

- ***J. Richmond*** - is creating an accurate representation of turbulence for the inlet of the model, details of this can be found in his I2 report [4].
- ***J. Mullins*** - is investigating the effects that topography has on wind profiles, in the hope that this information can be included in simulations. Details of this can be found in his I2 report [5].
- ***J. Morgan (this report)*** – is investigating the different ways of modelling turbulence inside a domain, showing the benefits and drawbacks of each.

Aims

1. To investigate the interactions of air with a static object such as a bridge and to understand the effects that these interactions can have.
2. To investigate the different ways of modelling turbulence.
3. To help create an accurate representation of air moving over the Humber Bridge.

Objectives

1. Choose a suitable turbulence model for modelling air past a bridge.
2. Carry out simulations on a well understood geometry and compare the simulation results with known experimental values.
3. Extract data from this simulation for use with the results of the structural subgroup.
4. Analyse data extracted from the Humber Bridge simulation.

Outcome of this Individual Project

This project should provide the structural subgroup with a range of frequencies at which a particular wind speed will cause the Humber Bridge to vibrate.

1.2. Summary of Previous work

In this work's corresponding I1 report, some of the basic concepts behind CFD were briefly looked at, including turbulent vs. laminar flow, creating the geometry of a domain, meshing, initial conditions, and boundary conditions [6]. The main bulk of the report however was an investigation into different types of turbulence models which can be employed in a simulation. The three types of modelling, direct numerical simulation (DNS), Reynolds averaged Navier-Stokes (RANS), and large eddy simulation (LES) were all studied.

DNS, a method of turbulence simulation which solves all Navier-Stokes and continuity equations for a particular problem, was shown to produce the highest simulation accuracy at the cost of a high computational expense. For almost all engineering applications DNS is completely impractical, requiring far more computing power than modern technology can provide. It does have its uses in fluid dynamics research and is sometimes used as a highly accurate comparison for other turbulence models.

A more realistic model (in terms of required computing power) is RANS modelling. In a RANS model the properties of fluid flow are split into two components; a time averaged component and a function representing the fluctuations of the fluid property with respect to time. Using this decomposition of fluid flow the RANS equations can be formed. The RANS equations use the averaged values of fluid property and one non-linear term called the Reynold stresses. The Reynold stresses arise as a result of the time dependent fluctuating component of fluid flow. Whilst the majority of the RANS equations can be solved easily, the non-linear nature of the Reynolds stresses mean that they must be modelled. There are many different ways of modelling the Reynolds stresses and the merits and drawbacks of the most common models have been covered in the I1 report [6]. Whilst RANS modelling can provide quick solutions to many problems it has the inherent disadvantage of only producing time averaged solutions. All instantaneous detail relating to the flow is lost. Unfortunately, vibration is a time dependent phenomenon, meaning that RANS modelling cannot be used to predict it.

RANS models, whilst providing accurate results for large numbers of cases, are by nature very generic and simulate all types of turbulence as the same. This is particularly problematic when looking at different sizes of eddies. The smallest eddies (Kolmogorov eddies) in a fluid flow are isotropic. Generally they all behave in a similar manner and are heavily influenced by

viscous forces. On the other hand, the largest eddies in a flow are heavily influenced by the eddy location, the surrounding geometry, pressure gradients, and bulk fluid velocity. When considering flow like this, it is hard to justify a one-size-fits-all model. LES aims to provide an alternative.

The large computational cost of DNS arises from resolving the smallest scales of fluid flow. These small scale eddies require incredibly high mesh resolution and a very small time step. LES avoids solving these incredibly computationally expensive scales by employing a filter function. This filter function is a spatial filter. Any eddies which are larger than the spatial filter are numerically resolved. Any eddies which are smaller than the filter function have all information related to them discarded. The discarding of this information causes an imbalance in the domain. These imbalances are represented by sub grid scale (SGS) stresses. These SGS stresses must be modelled.

As LES does not use any time averaging, instantaneous details about the flow can be determined. As such it can be used to model vibrations. Unfortunately LES suffers many drawbacks when compared to RANS modelling. LES requires a much finer mesh than RANS, and as a consequence a much smaller time step is required. This greatly increases the computational time of LES, meaning that simulations can easily take days or weeks to complete. The information summarised above, can be found, in detail, in this report's corresponding I1 report [6].

1.3. Structure of this Report

Section 2 – An investigation of wind induced vibrations, focusing on vortex shedding. It will cover the different types of vortex shedding and the effects that they can have on bluff bodies. Methods of vortex suppression are also studied.

Section 3 – An investigation into different types of LES modelling, and a description of how the project simulations were setup.

Section 4 – The presentation and analysis of the simulations carried out

Section 5 – A conclusion of the report with suggestions for further work.

Section 6 – Project management, health & safety, and sustainability

Section 7 – The contribution of this individual report to the group, highlighting collaboration methods and suggestions for future work.

2. Literature review

One method by which wind loading can cause damage is aeroelastic flutter. Aeroelastic flutter is caused by positive feedback between an elastic object and wind loading. There are other mechanisms by which wind loading can cause damage. One of these mechanisms is wind induced vibrations. These vibrations are mostly caused by vortex shedding. Vibrations are hugely problematic for engineers, as it causes fatigue. Additionally, if the vibrations coincide with the natural frequency of an object, then resonance can occur. This can potentially be disastrous. For this reason it is important that vortex shedding is properly understood and accounted for.

When flow with a sufficiently high Reynolds number passes over a boundary, vortices are shed [7]. A vortex is a description of fluid motion where the flow is mostly rotating around an axis. The shedding of vortices causes a force to act on the boundary from which it is shed. Due to the nature of fluid flow, vortex formation and shedding can often be periodic [8]. The most well-known type of vortex shedding is called the Von Kármán vortex street. This type of vortex shedding is found in the wake of bluff bodies (non-streamlined objects such as those with circular or square cross sections). This type of vortex shedding is characterised by periodic, alternating, asymmetrical vortices. *Figure 2-1* shows a Von Kármán vortex street. As the image shows, the vortices are shed alternatively, with the top vortices rotating in a clockwise direction and the bottom vortices rotating anti-clockwise. These types of vortices are named after Theodore Von Kármán for his work in the field [9].

When fluid flows past an object, streamlines are formed parallel to the wall. For a streamlined body these streamlines will follow the wall until reaching the tail of the body where they will continue into the flow. For a bluff body these streamlines will at some point separate from the wall. This can be seen in *Figure 2-2*. This separation will create a region of low pressure. This creates a pressure difference across a body which will impart a force on the body. The formation of a vortex is due to the separation of the streamline from the body and the consequent motion of fluid into the low pressure region. Von Kármán was the first to show that vortex shedding was the most stable when it happened in an asymmetrical, alternating manner.

He also showed that the shedding of vortices was only stable for a certain ratio of distance between rows of vortices and vortices within rows. In addition to this he showed that the mechanism behind vortex drag was linked to the momentum which was carried by a vortex [10].

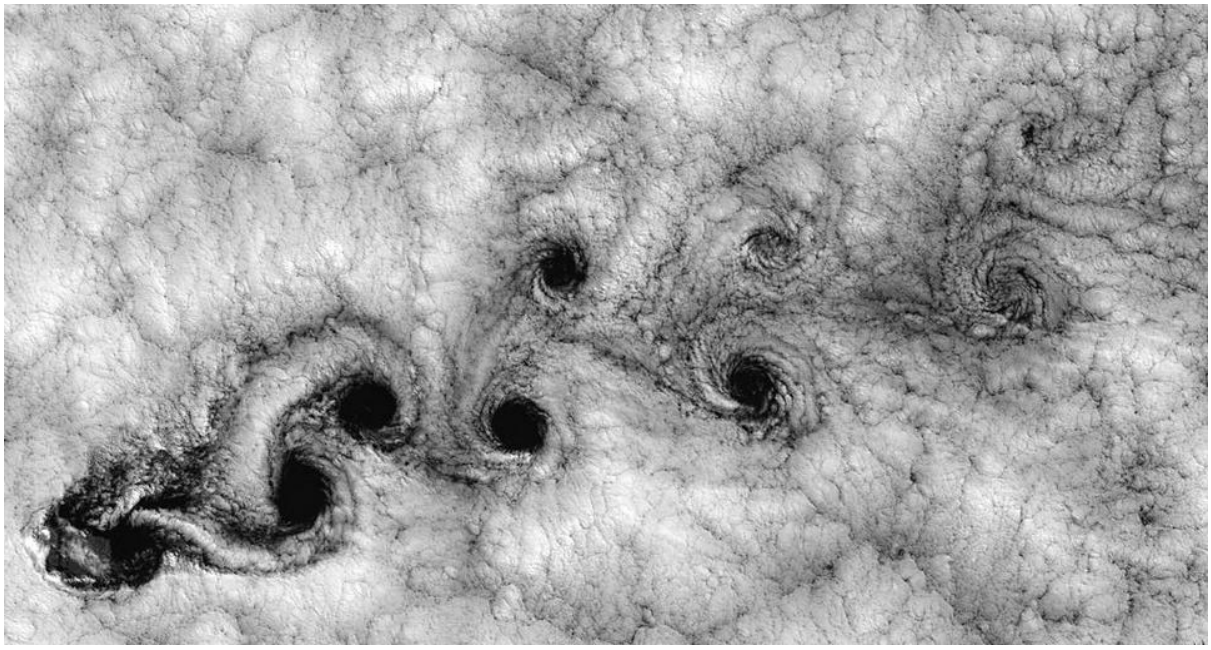

Figure 2-1 Picture, taken by the Landsat 7, of clouds off of the Chilean coast near Juan Fernandez Islands. The clouds are showing a Von Kármán vortex street. Image taken from [11].

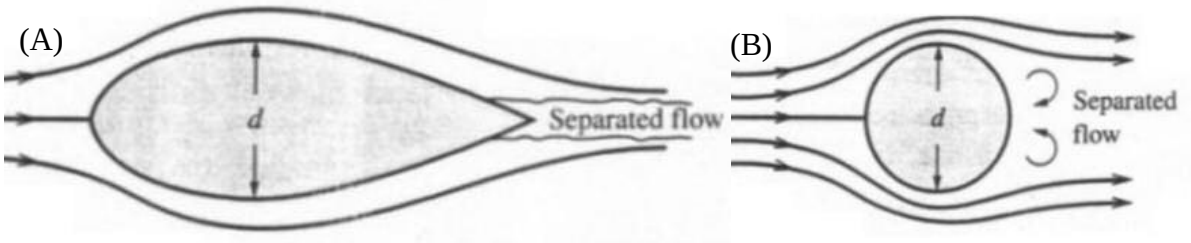

Figure 2-2 - Schematic diagram of two bodies, showing the streamlines going past them (A) a streamlined body (B) a circular cylinder. Image taken from [12].

Other studies have shown that it is possible to control the size and energy of the Von Kármán vortex streets. An important part of the formation of the vortex street is the stagnation region. This is the area of fluid downstream of a bluff body which is in direct contact with the wall. The addition of physical barriers in this region, such as splitter plates, has been shown to effectively reduce the strength and alter the frequency of the vortex street [13]. As such this can be an effective tool in reducing the size of oscillations on structures such as bridges. Conversely researchers have also shown that with careful control of geometry, splitter plates can also be used to increase both the frequency and strength of Von Kármán vortices [14].

Whilst the Von Kármán vortex street is by far the most common type of vortex shedding, other forms of vortex shedding can also present issues for bridges. Von Kármán vortex streets are classed as a two shear layer shedding mechanism. If a set of Von Kármán vortex streets (or any other input) is strong enough to cause an object to heave, then a special type of single shear layer vortices can introduce a secondary vibration.

Due to the complex geometry of structures such as bridges, the vortex patterns can also be quite complicated. In order to better understand the physics behind vortex shedding, geometries are often simplified to have square or rectangular cross sections. In one experiment a rectangular cylinder with a length to height ratio of 8.2 was placed in a low velocity flow and was forced into a heaving motion. The researchers showed that two different types of single shear layer vortices were formed [15].

The first vortex formed at the leading edge, and was convected along the side of the body towards the trailing edge. The researchers measured the convection speed of this vortex to be 60% of the bulk velocity. The formation of this vortex will have exerted a force on the square cylinder causing it to move. This motion induced a secondary single shear layer vortex at the trailing edge. When the vortex formed at the leading edge convected to the trailing edge, the primary and secondary vortices were shown to coalesce. This formed a vortex with enough momentum to be shed from the structure. This coalesced vortex caused an even greater force, this time at the trailing edge. The repeated heaving motion of the bluff body will cause this process to repeat, thus, creating an additional periodic force on the object [15].

It is important to determine if these single shear layer vortices are related to the Von Kármán vortex streets. By installing splitter plates near the wake of the rectangular cylinder, the Von Kármán vortex street can be suppressed to near non-existence. Regardless the vortices still formed on the leading edge of the bluff body and travelled at 60% of the bulk velocity. This is a good indication that the formation of these primary single shear layer vortices is unrelated to the flow in the wake. As an additional point of interest, with the splitter plates installed, the trailing edge vortices did not form. This vastly reduced the force created by the single shear layer vortices [15]. This type of vortex shedding has been called low-speed vortex excitation [16]. Vortices formed by this mechanism are restricted in size by the geometry and the size of

the heave, not the fluid velocity; hence, they are unlikely to cause catastrophic failures. Nevertheless they should be considered when investigating fatigue.

A Von Kármán vortex street is a two shear layer, asymmetrical, vortex mechanism. It is also possible to achieve a similar two shear layer, symmetrical, vortex shedding mechanism (see *Figure 2-3*). This mechanism can appear at low fluid velocities, meaning it is likely to occur on bridges. This type of vortex mechanism occurs when a bluff body is exposed to a fluctuating flow. The symmetrical vortices were shown to form when the flow velocity had a r.m.s value of as little as 1% of the bulk velocity [17]. Additionally, this symmetrical vortex pattern can occasionally evolve into an amplified Von Kármán vortex street. This amplified vortex street can cause a drastic increase in the drag of an object [18].

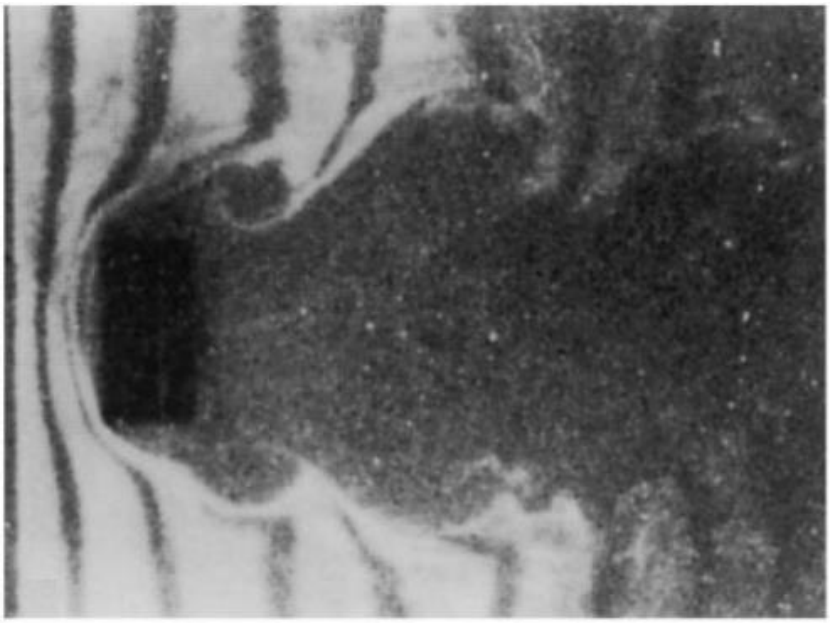

Figure 2-3 - Image of a symmetrical vortex pattern in the wake of a rectangular cylinder. Image taken from [19].

Engineers will try to design the cross section of bridges so that the different types of vortex shedding described above can be mitigated. One common bridge deck cross section is the trapezoidal box girder deck. The Humber Bridge has a slightly modified version of this deck. In recent years, after carrying out wind tunnel tests, researchers have found that "vortex shedding can be avoided or kept at insignificant levels if the angle between the horizontal extension of the bottom plate and the lower inclined panels is kept at $15^{o"}$ [20]. An example of a trapezoidal box girder deck with an angle of 14.7^{o} can be found in *Figure 2-4*. The researchers

have stated that this type of geometry is more streamlined; consequently, there is no fluid separation and vortices cannot form.

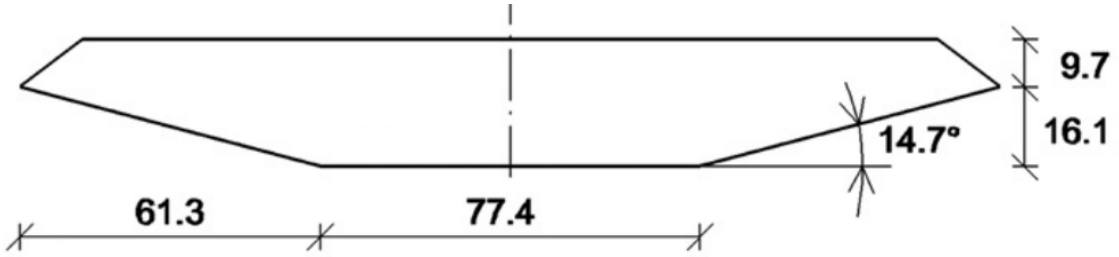

Figure 2-4 - Schematic diagram of a trapezoidal box girder deck, showing a 14.7^0 angle. This would indicate that this bridge would not shed vortices. Image taken from [20].

After testing multiple angles the researchers determined that an angle of approximately 15^o showed the most consistent reduction of vortex shedding across a large range of Reynolds numbers. The researchers continued their work by adding barriers to the bridge deck, to determine if they would decrease the streamlining. The two different types of barriers the researchers used are shown in *Figure 2-5*. The authors found that at some angles the addition of these open barriers would introduce vortex shedding, where previously the shedding had been suppressed. For the researchers' final simulations, they mimicked the effects of heavy snowfall. They turned the barriers from open barriers to solid walls (to mimic an open barrier covered in snow). The researchers found that the solid barriers disrupted the streamlining of the bridge enough to introduce vortex shedding for all angles [20].

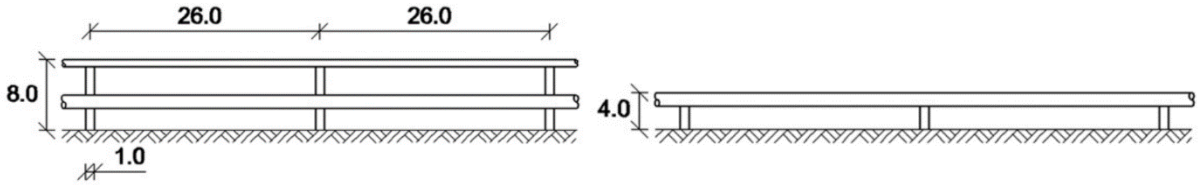

Figure 2-5 - Schematic drawing of the two barriers tested in the wind tunnels, (A) Railing (B) Median divider. Image taken from [20]

The author of this I2 report has identified an area for further research. Whilst the researchers tested the effects that barriers have on the suppression of vortices, they did not test the effects that vehicles have. In heavy traffic conditions, or in traffic jams where vehicles are near stationary, the traffic may act in a similar manner as the solid barriers. In this respect, the addition of traffic to the wind tunnel testing may result in vortex shedding, once again, appearing at all angles.

3. Theoretical Background & Experimental Design

Having gained some understanding of how wind loading can cause vibrations, it is important that these vibrations be correctly modelled. In the I1 report a large investigation was carried out into types of RANS modelling [6]. Ultimately it was decided that LES modelling is the most appropriate choice for modelling vibrations. In this section the theory behind different types of LES are explained, with their benefits compared. Also included in the I1 report were initial simulations. The simulations were of a widely studied case called the square cylinder case. This geometry has large amounts of experimental and numerical data for a wide range of Reynolds numbers; as such, it is often used as a verification case. In the I1 simulations, different RANS models were correctly implemented, and were compared to experimental and numerical results. The second half of this section will continue from the I1 report. It will showcase LES simulations of the square cylinder which have been carried out, and will explain the simulation choices.

3.1. Smagorinsky-Lilly SGS Model

The mathematical principles behind LES were first proposed in 1963 by Joseph Smagorinsky in an attempt to simulate atmospheric air currents [21]. However it was not until 1970 that James Deardorff expanded on this, creating some of the more recognisable features of modern LES [22]. In this paper Deardorff showed that after spatially filtering fluid flow in three dimensions, the SGS stresses in a flow could be related to the local rate of strain of the resolved flow (an idea initially proposed by Smagorinsky [21]). Using this idea Deardorff created a SGS model of the SGS stresses, which included terms for an SGS viscosity and a dimensionless constant called the SGS constant (C_{SGS}). Being a dimensionless constant, it should remain constant for all types of flow. Previously in 1967 Douglas Lilly conducted a theoretical analysis of the decay rates of isotropic turbulent eddies [23], using this work the value of C_{SGS} was found to be in the region of 0.17. This SGS model is now known as the Smagorinsky-Lilly model and was the basis for LES simulations for a while.

The Smagorinsky-Lilly model was shown to be inaccurate in certain situations. The basis for these inaccuracies was found to be the value of $C_{SGS.}$ Several researchers showed that the value of C_{SGS} changed depending on the application which LES was being used for. A review of advances in the Smagorinsky-Lilly model carried out in 1984 showed that the value of C_{SGS}

ranged from 0.10-0.24 [24]. This variance in C_{SGS} demonstrated that the behaviour of the Kolmogorov eddies was not as uniform as was first proposed. This meant that when using LES the constant would have to be determined experimentally for each simulation, or an approximation would have to be made.

3.2. Dynamic SGS Model

One of the main issues with the Smagorinsky-Lilly model is an assumption made about the energy cascade. In fluid dynamics, the energy cascade is the movement of energy from the largest eddies in a domain to the smallest. The largest eddies are formed by the shear stresses in the bulk flow. These largest eddies are very unstable and will break up into smaller eddies, passing on their associated energy in the process. At this scale, eddies are still dominated by forces such as pressure gradients and shear stresses. The process of breaking up and passing on energy to smaller eddies will repeat itself until the Kolmogorov sized eddies are formed. At this scale viscous forces dominate the flow, and energy is dissipated as heat.

The Smagorinsky-Lilly model makes the assumption that the movement of energy in this process is only in one direction (from large eddies to small eddies). As was demonstrated in 1979, this is not the case. Whilst the net movement of energy is from the largest to smallest eddies there is a backscatter of energy in the opposite direction [25]. More recently, DNS simulations have shown that the SGS stresses calculated in LES are quite different to the actual SGS stresses [26,27]. The difference is thought to have arisen as a result of the un-modelled backscattered energy.

Smagorinsky's original idea that the SGS stresses are related to the local rate of strain for the whole flow can be improved upon with a small change. Instead of relating the SGS stresses to the local rate of strain of the entire flow, the SGS can be related to the strain of the smallest resolved eddies. This can be implemented through the use of multiple filters. The first filter is the regular spatial filter used by the Smagorinsky-Lilly model. The second filter, is a spatial filter, twice the size of the first. This second filter will filter out the smallest resolved eddies. The strain in these eddies can be determined and used to calculate the value of the SGS stresses. This method of modelling the SGS stresses was compared to DNS and was deemed to be more accurate, as it did not require tweaking of C_{SGS} [28]. In its early stages this method showed signs of instability. This instability was overcome with the addition of a dampening function

[28]. This model was tweaked in 1991 producing a revised version of the model, now known as the dynamic SGS model [29].

3.3. Y^+ Values and the Boundary Layer

In CFD it is common to use the dimensionless wall unit, y^+. Calculating y^+ values can be done using *Equation (1)*. Where U_{fr} is the friction velocity at the nearest wall, y is the vertical distance to the nearest wall and ν is the kinematic viscosity. These dimensionless wall units are particularly useful when talking about the boundary layer of a flow and when discussing the meshing of a domain.

$$y^+ = \frac{U_{fr}\, y}{\nu} \qquad \textit{Equation (1)}$$

A schematic diagram of a boundary layer is shown in *Figure 3-1*. This diagram shows that a boundary layer is comprised of two general sections; the outer layer and the inner layer. The inner layer is comprised of three sections; the log-law layer, the buffer layer, and the viscous sublayer. The viscous sublayer comprises of fluid in which $y^+ \leq 5$. In this region the relationship between U^+ (a dimensionless velocity unit, calculated in a similar manner to y^+) and y^+ is linear. In this region viscous forces dominate the flow. The log-law region of fluid is the region in which $y^+ \geq 30$. In this region the relationship between U^+ and y^+ is logarithmic. Fluid in this region is dominated by inertia forces. Fluid in between these two regions ($5 < y^+ < 30$) is called the buffer layer, and can be thought of as a transitional region.

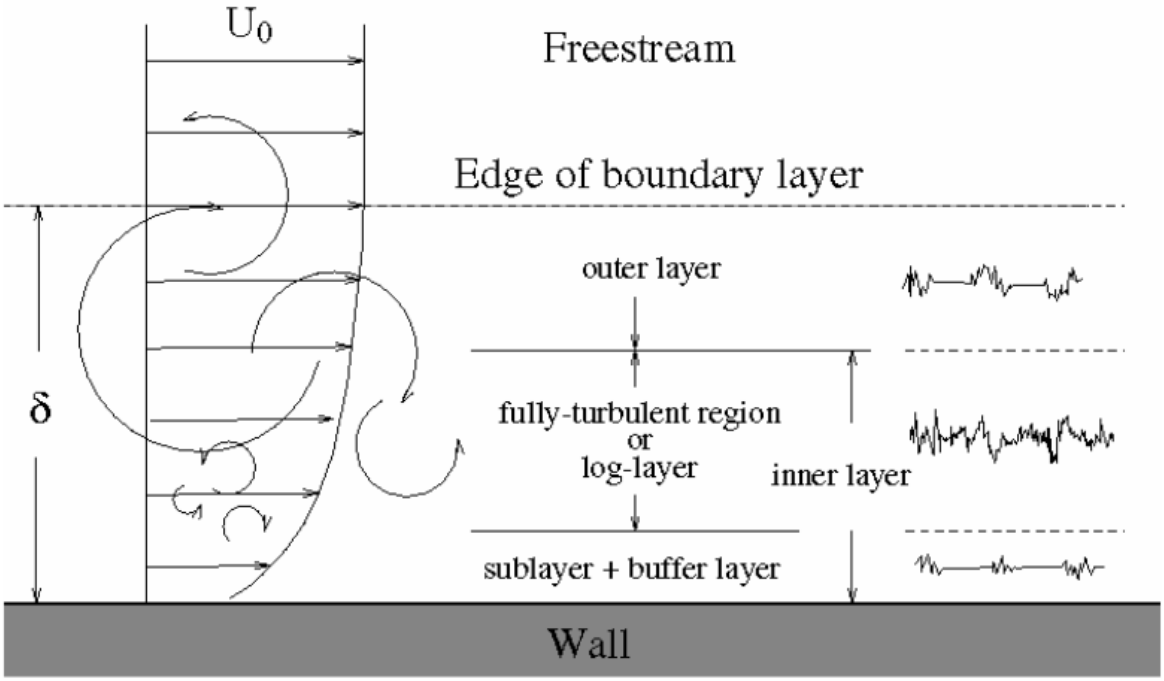

Figure 3-1 - A schematic diagram of a boundary layer. Image taken from [30].

3.4. Detached Eddy Simulation

In fluid flow turbulence is caused by shear stresses. Objects which are stationary, with fluid moving past, create shear stresses in the flow. This shear stress causes a boundary layer to form. This boundary layer can be thought of as a source of turbulence generation. The high computational cost of LES arises due to the meshing requirements of these boundary layers. By nature, a single cell is only allowed one associated velocity. This makes the modelling of boundary layers (where velocity reduces from the free stream velocity to zero) problematic. For LES to work accurately, the cells next to the wall must have a $y^+ \leq 1$. If the cells have a $y^+ > 1$ then the boundary layer will be incorrectly modelled and inaccuracies will arise.

As was shown by Blasius in 1908, the thickness of a boundary layer (δ) over a flat plate can be calculated using *Equation (2)* [31]. Where x is the distance downstream from the start of the boundary layer. It should be noted that as Reynolds number increases, the size of the boundary layer decreases. At low Reynolds numbers achieving a mesh where the first cells have a $y^+ \leq 1$ is not an issue as the boundary layers are quite large. At higher Reynolds numbers the boundary layer gets smaller. As a consequence achieving a $y^+<1$ requires a finer mesh.

$$\delta = \frac{0.382x}{Re^{\frac{1}{5}}} \qquad \textit{Equation (2)}$$

In LES, the filtering function that is used means that all cells in a domain must be of the same size. This becomes problematic when the Reynolds number becomes large. If the boundary layer thickness halves, then the height of the smallest cell must also half. However as the cells ideally need to remain cubic, the cell size must also reduce in the other two axes. Thus, if the boundary thickness of a wall halves, then the number of required cells increases eightfold.

In addition to this, the maximum Courant number of a domain must remain below 1. The Courant number is a dimensionless number which indicates how many cells a particle of fluid moves through per time step. If the Courant number is above 1 then the fluid particle is skipping cells. This can cause a simulation to crash. A schematic diagram with a short explanation of courant numbers can be found in *Figure 3-2*.

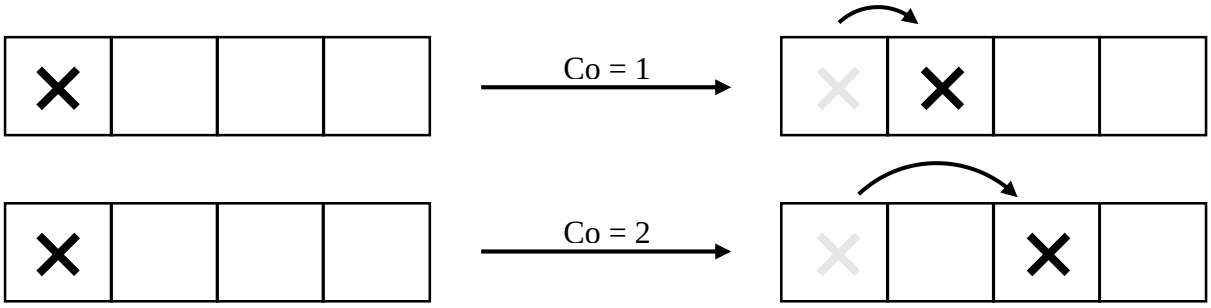

Figure 3-2 - Schematic diagram demonstrating Courant numbers. In the top image the fluid particle (indicated by an X) moves through one cell per time step, as such it has a Co = 1. In the bottom image, the particle of fluid moves through two cells per time step and has Co = 2

The equation for calculating Courant numbers can be found in *Equation (3)*, where Δt is the time step and Δx is the length of one cell. For the Courant number to remain constant, if the cell size halves, then the time step must half to compensate. In summary to accurately model a boundary layer which has been halved in size, requires eight times as many cells and twice as many time steps. Assuming a linear relationship between cell number, time step, and computational time, this would mean a sixteen fold increase in simulation time.

$$Co = \frac{U\Delta t}{\Delta x} \qquad \text{Equation } (3)$$

In aerospace applications Reynolds numbers often easily reach into the millions causing very small boundary layers. Estimations by Spalart suggest that a mesh containing 10^{11} cells with 10^{7} time steps would be required for most aerospace applications which use LES. With advances in computational power increasing at the current rate, he predicted that it would be possible to start simulations of that size in approximately 2045 [32]. Engineers however needed a CFD model which could predict time dependent phenomenon in a reasonable time frame. For this reason Spalart, in 1997, created a hybrid model of RANS and LES modelling [32]. This modelling, which is called detached eddy simulation (DES), aims to combine the accuracy and time dependent nature of LES with the speed of RANS modelling.

DES works by switching between RANS and LES. In regions where the mesh is fine enough to perform LES, LES is used. In regions where the mesh is not fine enough for LES, a variation on the Spalart-Allmaras RANS model is used. In practice, this means that in areas of massive fluid separation (where little mesh refinement is needed) LES is used, and near the boundaries (where large refinement is required) RANS modelling is used. The initial DES model was based exclusively off of the one equation Spalart-Allmaras model however it has since been developed to use other types of RANS modelling [33].

To implement DES a switching function is required. This switching function determines if LES or RANS will be used in a particular region. Whilst it is easy to create this switch for the two extreme situations mentioned, it is harder to control in the grey areas in between. This issue is the largest criticism of an otherwise very useful turbulence model and is the reason why the model has been developed.

3.5. Delayed Detached Eddy Simulation

The switching function in DES is based on the relationship between the cell size, Δ (Δ ≡ max (Δx, Δy, Δz)), and the distance to the nearest wall. As such it is dependent on the mesh. *Figure 3-1* shows three typical meshes. Mesh (A) is very typical of a DES mesh. In this mesh the value of Δ is large enough so that RANS modelling will be used throughout the boundary layer. Mesh (C) is typical of a LES mesh. This mesh is fine enough to allow for full LES throughout the boundary layer. Mesh (B) is ambiguous and will cause problems for DES. The issue with this mesh is that the switching function will activate at an incorrect position within the boundary layer. This causes a reduction in eddy viscosity. Consequently this reduces the modelled Reynolds stresses, without compensating with an increase in resolved Reynolds stresses [34].

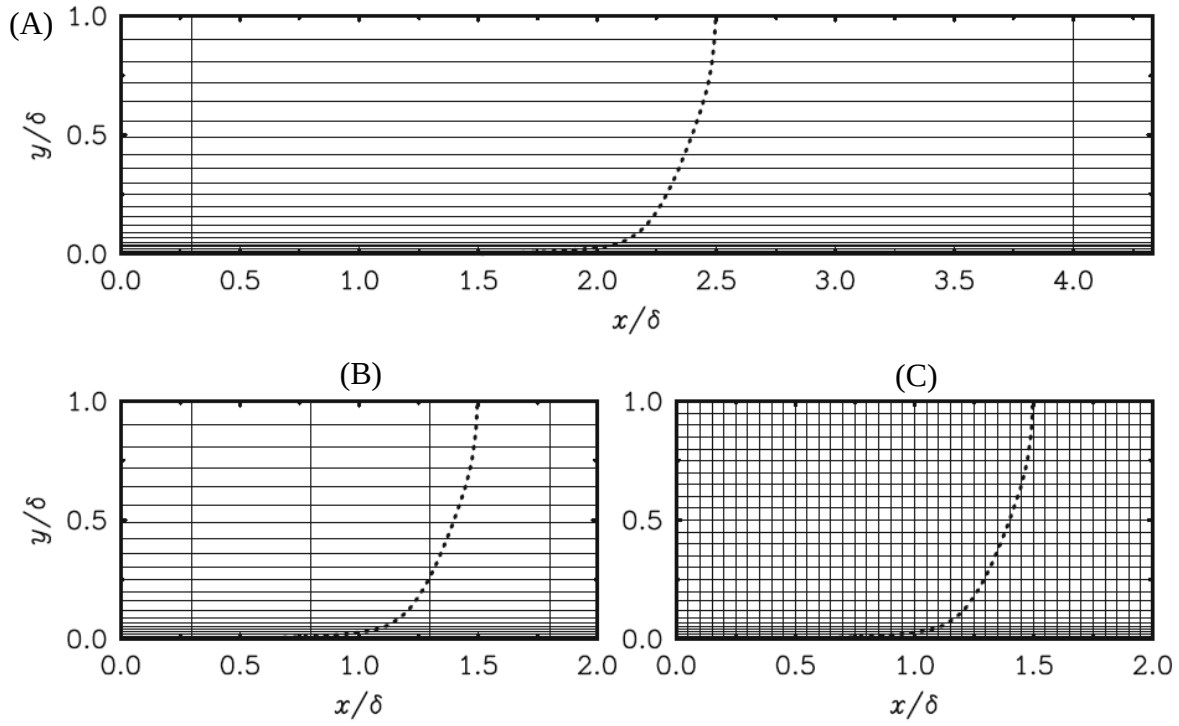

Figure 3-3 - Image showing three different types of mesh. (A) A typical DES mesh, (B) An ambiguous mesh (C) A typical LES mesh. Image taken from [34].

Delayed detached eddy simulation (DDES) proposes that this switching method is not optimal. DDES is based on the idea that the switching function should also detect the boundary layer, and should delay the full effects of RANS mode, even if the cell size would activate the DES switch. The detection of the boundary layer is dependent on the eddy viscosity. This means that the switching device is dependent on the previous time steps solution, hence the name delayed DES [34]. The use of DDES has been thoroughly tested and experts believe that DDES is likely to become the standard version of DES [35].

3.6. LES Modelling of the Square Cylinder Case

The simulations presented here are a direct continuation of the simulations presented in the I1 report [6]. The geometry and all physical parameters of the problem have remained consistent, with the only changes being the method of turbulence modelling. To remind the reader, the geometry for the case is shown in *Figure 3-4* and is based on a similar simulation carried out by researchers [36].

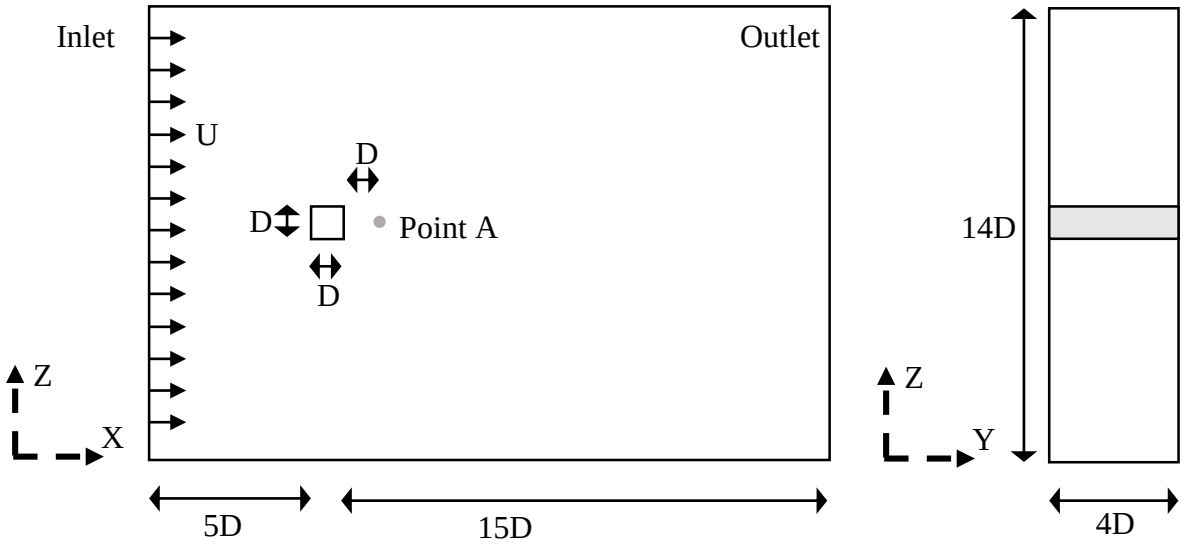

Figure 3-4 Geometry of the square cylinder case, showing dimensions, axes, locations of the inlet & outlet, and the uniform velocity profile.

The value of D is 0.04m. The domain was meshed so that all cells were of equal size in all directions with 6 cells per unit length D. After the inlet and outlet faces had been specified, the square cylinder had its boundaries set as walls. All remaining faces were symmetry functions. The velocity was set so that the inlet produced a mean velocity of $U=0.535ms^{-1}$. The kinematic viscosity, $\nu = 1x10^{-6}m^2s$ and the characteristic length scale was 0.04m (D). This gave a Reynolds number of 21,400. These values were chosen so that this simulation could be compared to experimental results [37,38].

LES with a Uniform Inlet

The first LES case was run with a uniform inlet speed of $0.535ms^{-1}$. As the simulation has such a low Reynolds number it was deemed unnecessary to use DES or DDES. Instead a standard Smagorinsky-Lilly model was used. The outlet was set so that the average pressure across the face was 0Pa. 10 seconds of flow was simulated with a time step of $\Delta t = 0.001s$. The simulation took just under 4 hours to complete.

LES with a Turbulent Inlet

After running this simulation, J. Richmond managed to create a turbulent inlet for the domain. Inaccuracies often arise in LES due to non-realistic inlet conditions. As such the simulation was run again with J. Richmond's improved, realistic inlet conditions. This simulation took just under 5 hours to complete.

3.7. Humber Bridge Group Simulation Setup

This simulation was the combined work of the CFD subgroup. The geometry of the domain is shown in *Figure 3-5*. The domain was meshed using a component of the program OpenFOAM, called snappyHexMesh. In the cells next to the bridge deck, the aim was to create a mesh that looked like the mesh shown in *Figure 3-3* (A). Despite the prolonged, best efforts of the three CFD subgroup members, it was not possible to create these elongated cells. Instead cubic cells were used throughout the domain with mesh refinement used in regions of importance. A single level of refinement was used in the wake region of the bridge, whilst four levels of refinement were used in the cells directly touching the bridge. *Figure 3-6* shows the entire mesh and *Figure 3-7* shows a close-up of the mesh next to the bridge. The total number of cells in the domain was 2,342,457.

The inlet of the domain was set to use a combination of J. Mullins and J. Richmonds work. A velocity profile was created and turbulent fluctuations were imposed on top. This inlet condition mimicked wind speeds of $1ms^{-1}$. The kinematic viscosity was set to $1.5x10^{-5}$ m^2s (air). The characteristic length was chosen to be the length of the deck, 28.5m. This gave a Reynolds number of 1,900,000.

The bottom of the domain, along with the bridge deck, were set as walls. The outlet of the domain was set so that the average pressure across the face was 0Pa. The sides of the domain used OpenFOAM's cyclicAMI boundary condition. This boundary condition can be thought

of as a portal; fluid that goes out one side of the domain, enters at the same relative point on the other side. The top of the domain was set as a slip plane with a velocity of 1 ms^{-1} in the X-direction.

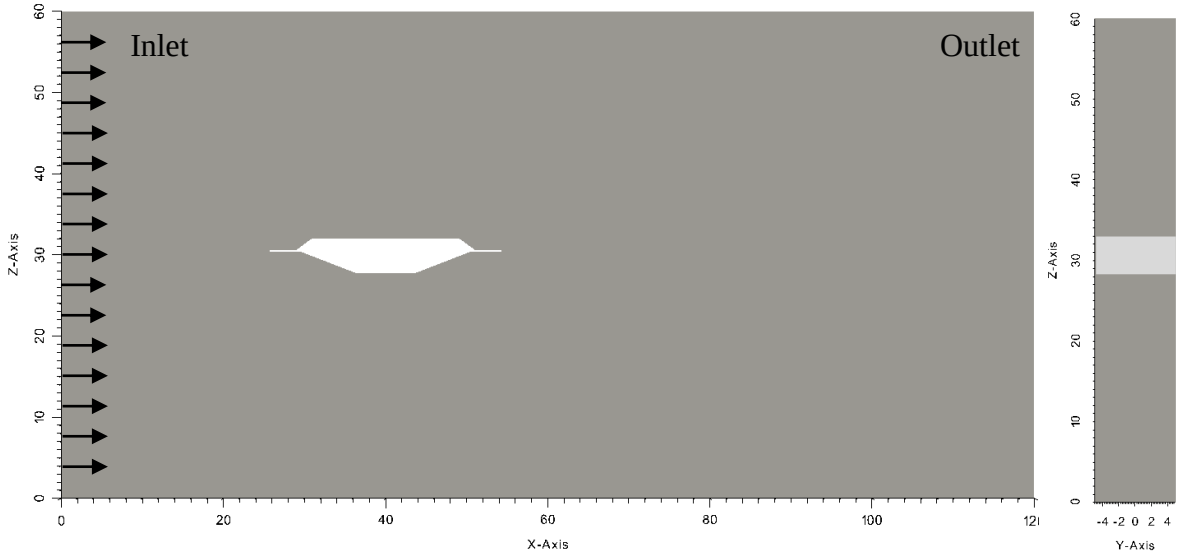

Figure 3-5 – Diagram of the Humber Bridge Simulation, showing dimensions, axes, and location of the inlet & outlet. All units in metres (m).

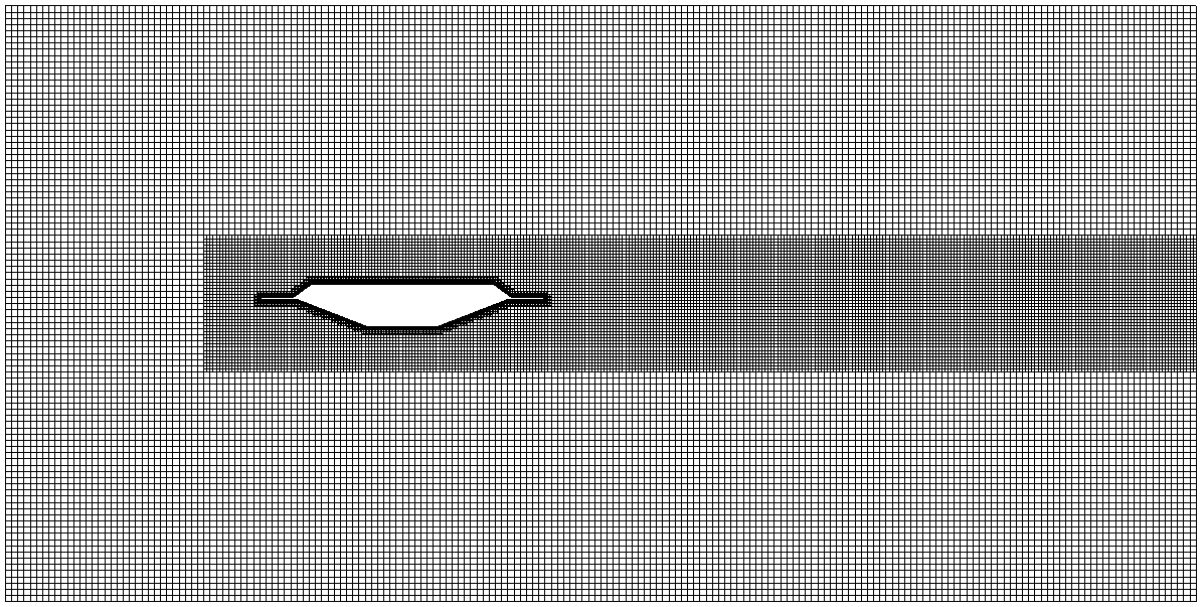

Figure 3-6 - Image showing the entire mesh. 1 level of mesh refinement has been used in the wake of the bridge, and 4 levels of refinement have been used in the cells surrounding the bridge.

As the model used varying sizes of cells it was not possible to use LES. DES would also not work with this mesh, as the cubic nature of the cells next to the bridge deck would cause the switching function to activate in incorrect regions. This leaves DDES as the turbulence model

of choice for this simulation. In total 315 seconds of air flow was simulated with a time step of 0.01s. This took 16.2 days to run.

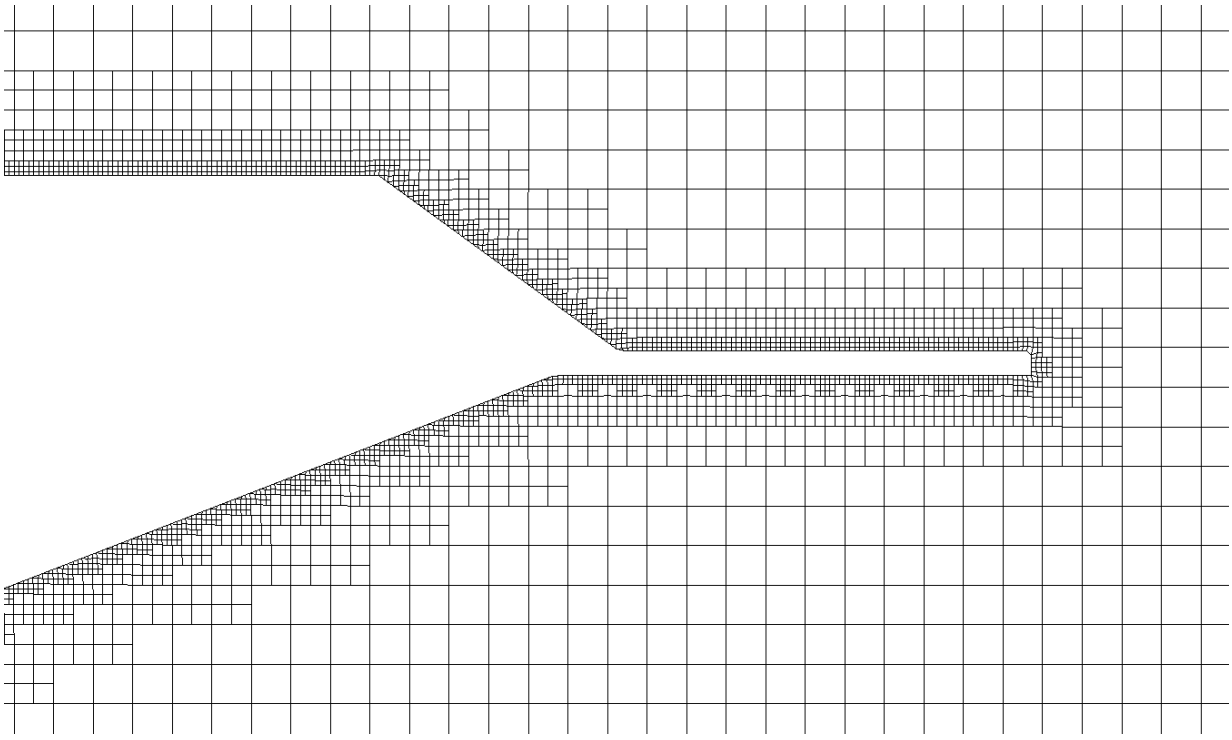

Figure 3-7 - Image showing a close-up of the mesh refinement next to the bridge.

4. Analysis of the Square Cylinder and Humber Bridge Simulations

4.1. Square Cylinder Simulation Results

The results of the first square cylinder simulation (with the uniform inlet condition) can be found in *Figure 4-1*, *Figure 4-2*, and *Figure 4-3*. The images show a velocity contour plot, force graph, and residual plot respectively. The results of the second square cylinder simulation (with the turbulent inlet conditions), can be found in *Figure 4-4*, *Figure 4-5*, and *Figure 4-6*, which show a velocity contour plot, force graph, and residual plot respectively.

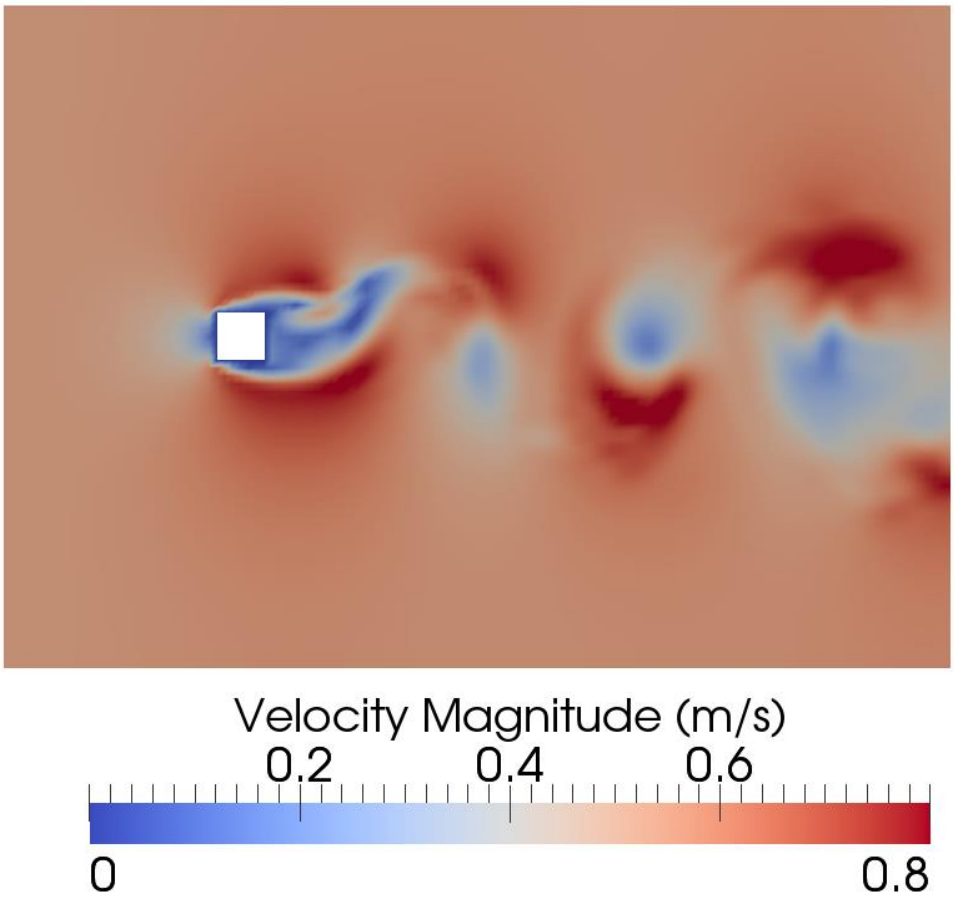

Figure 4-1 - Velocity magnitude contour plot for the square cylinder case with a uniform inlet.

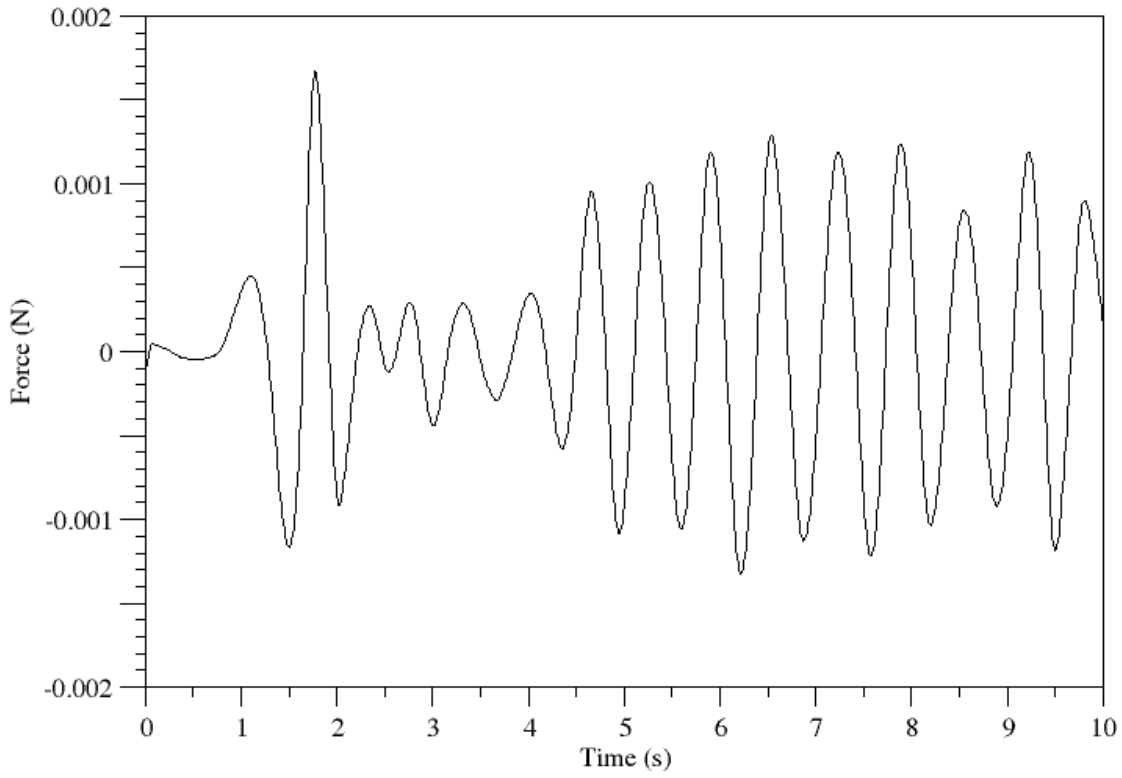

Figure 4-2 – Lift force on the square cylinder for the uniform inlet simulation.

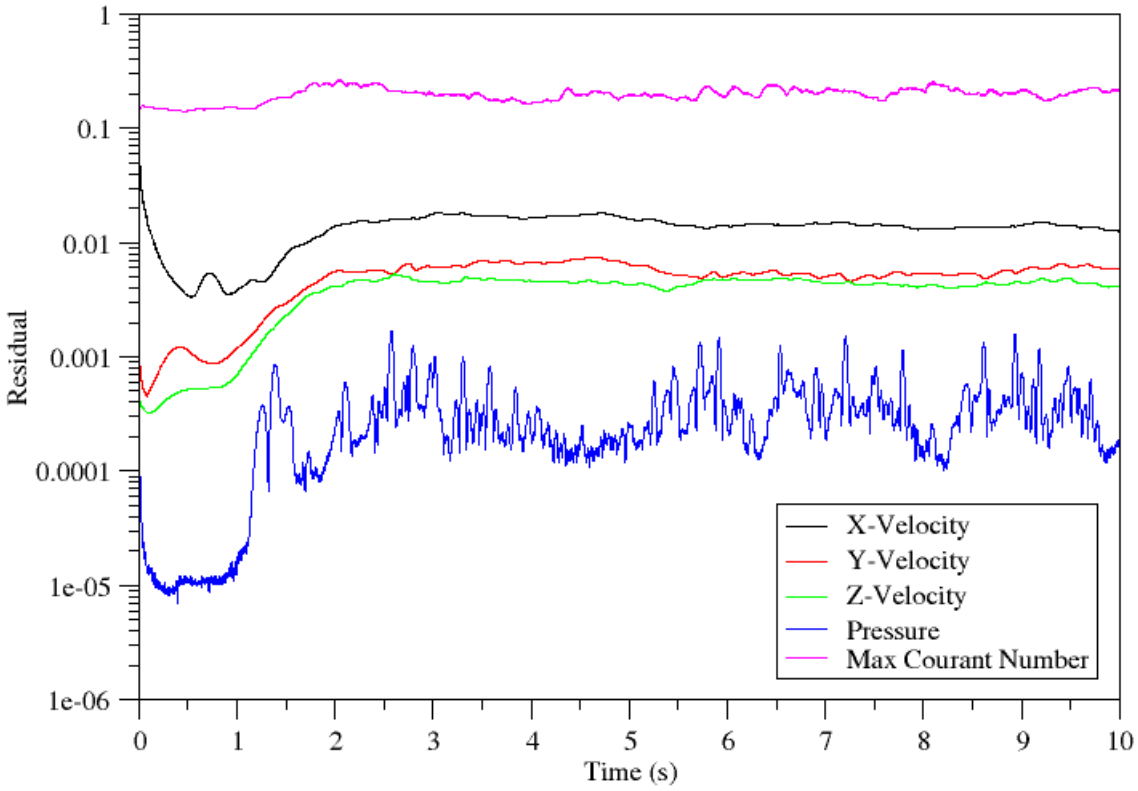

Figure 4-3 – Residual plot for the square cylinder case with a uniform inlet.

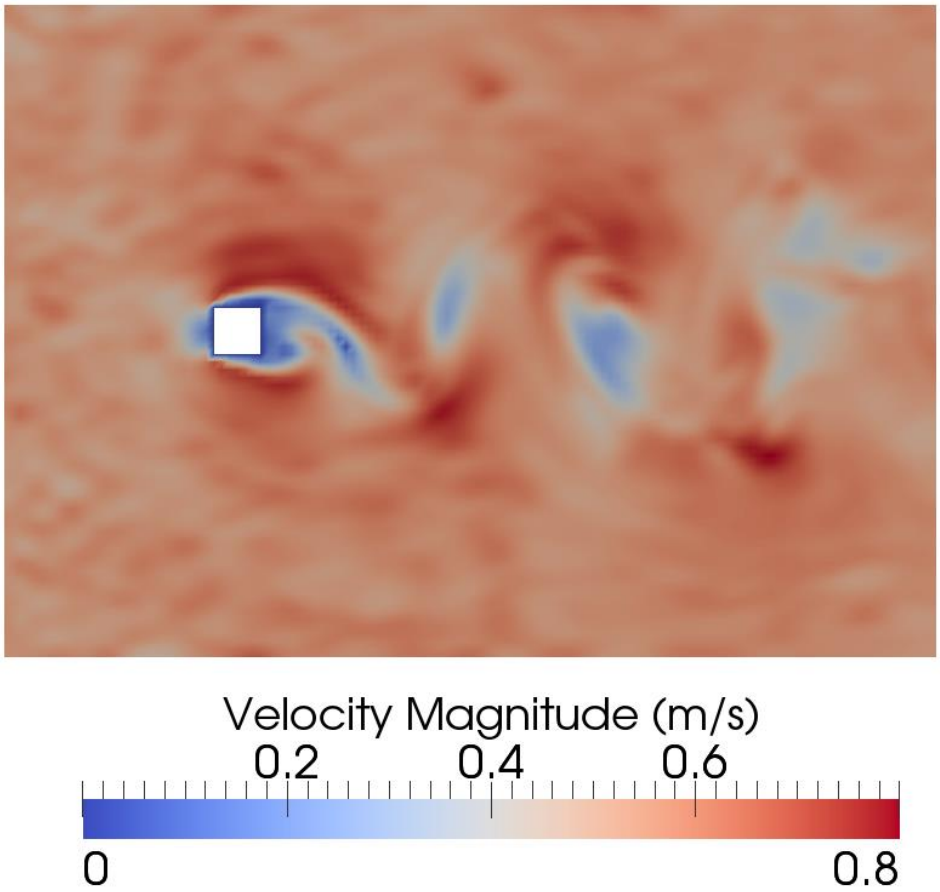

Figure 4-4 - Velocity magnitude contour plot for the square cylinder case with a turbulent inlet.

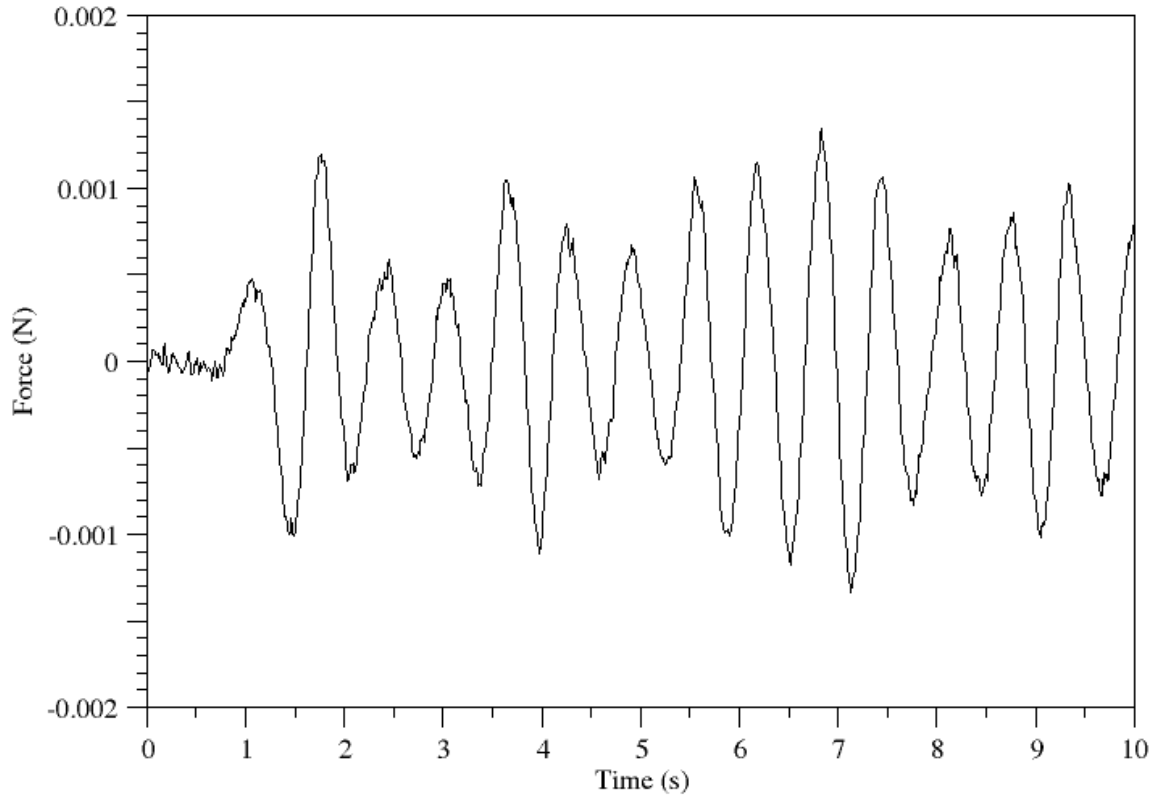

Figure 4-5 – Lift force on the square cylinder for the turbulent inlet simulation.

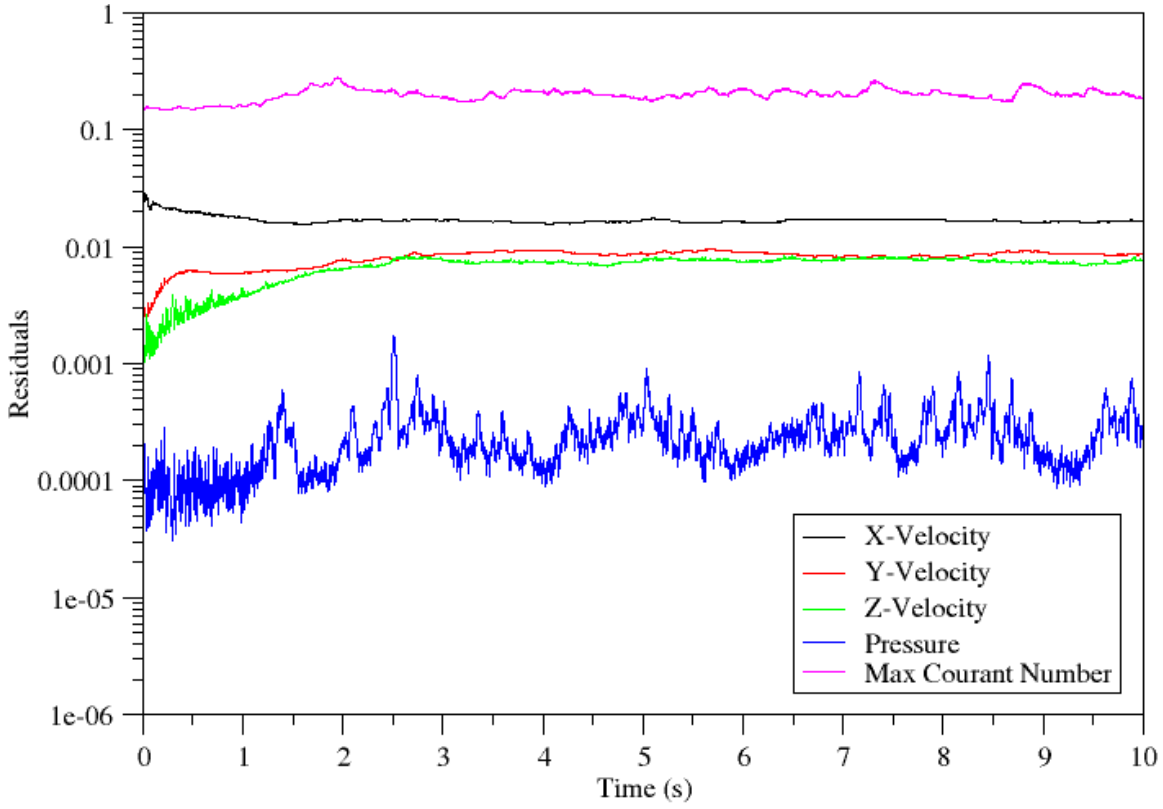

Figure 4-6 – Residual plot for the square cylinder case with a turbulent inlet.

4.2. Analysis of Square Cylinder Simulation Results

From the first glance, both *Figure 4-1* and *Figure 4-4* show that both simulations were successful at simulating vortex shedding. In both images the characteristic alternating swirls of a Von Kármán vortex street can be seen. The force graphs in *Figure 4-2* and *Figure 4-5* are also strong indicators that vortex shedding has been successfully simulated; both graphs show strong oscillations with a constant frequency. The residual graphs in *Figure 4-3* and *Figure 4-6* show that the simulations were both stable and indicate convergence. The maximum Courant number in both simulations reached 0.22 at their peaks; ensuring simulation stability. The pressure residuals in both reduced and stabilised at the low value of $1x10^{-4}$ with velocity residuals slightly higher at $1x10^{-3}$. This along with the consistent frequency of the force graphs would suggest that the simulations both converged.

As was previously stated experimental data is available for this geometry and Reynolds number. Experimental data shows that the shedding frequency of the vortices is in the range of 1.77±0.05Hz [37], or 1.79±0.05Hz [38]. Comparing these results with the simulations here does not yield great results. The first simulation, with the uniform inlet, has a shedding frequency of 1.52Hz, 15% off the actual value. The use of a turbulent inlet has improved these results, unfortunately they are still wrong. The second simulation was slightly better with a shedding frequency of 1.58Hz, 12% below the actual value.

In the I1 report an identical simulation was carried out using RANS modelling and the correct shedding frequency of 1.77Hz was produced [6]. This indicates that the LES simulation was incorrectly set up. Knowing that the geometry and physical parameters are correct, and also knowing that Courant number and residuals indicate both a converged and stable solution, a logical assumption would be that the mesh is not good enough. For LES to work the cells next to the wall must have a $y^+ \leq 1$. Unfortunately y^+ values can only be calculated after a simulation has been carried out. *Figure 4-7* show that the y^+ values next to the wall are far higher than they should be. This is undoubtedly the reason for the large error in shedding frequency.

To correct this, the mesh would need to be refined. Currently the y^+ values are much higher than they should be, suggesting that multiple levels of refinement are needed. As was previously stated in section 3.4, halving the cell height in LES will cause the simulation to run for sixteen times as long. The 5 hour simulation would turn into a 3 day simulation, and even

then the refinement may not be good enough. In the end it was deemed that refinement and improvement of the square cylinder case would not be a good use of time. Instead time would be better spent working on the Humber Bridge deck simulation.

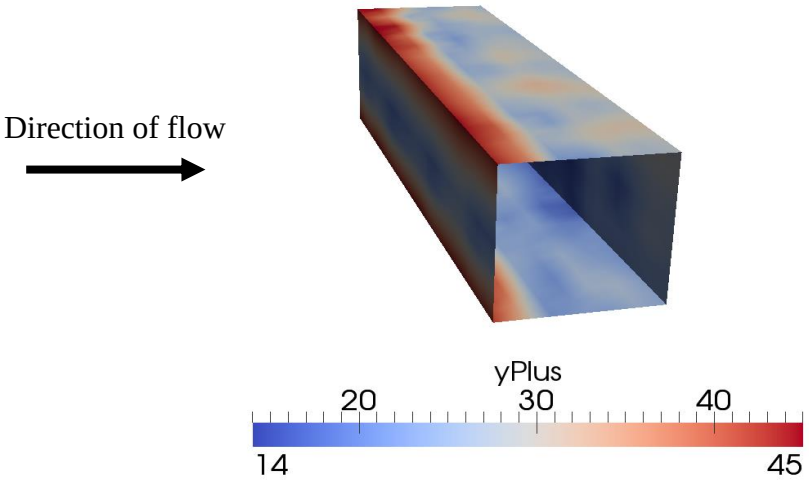

Figure 4-7 - A contour plot showing the y^+ values of the cells next to the wall.

4.3. Humber Bridge Simulation Results

The results of the Humber Bridge simulation can be found in *Figure 4-8*, *Figure 4-9*, *Figure 4-10*, and *Figure 4-11*. The images show a velocity contour plot, another velocity contour plot, a force graph, and residual plot respectively.

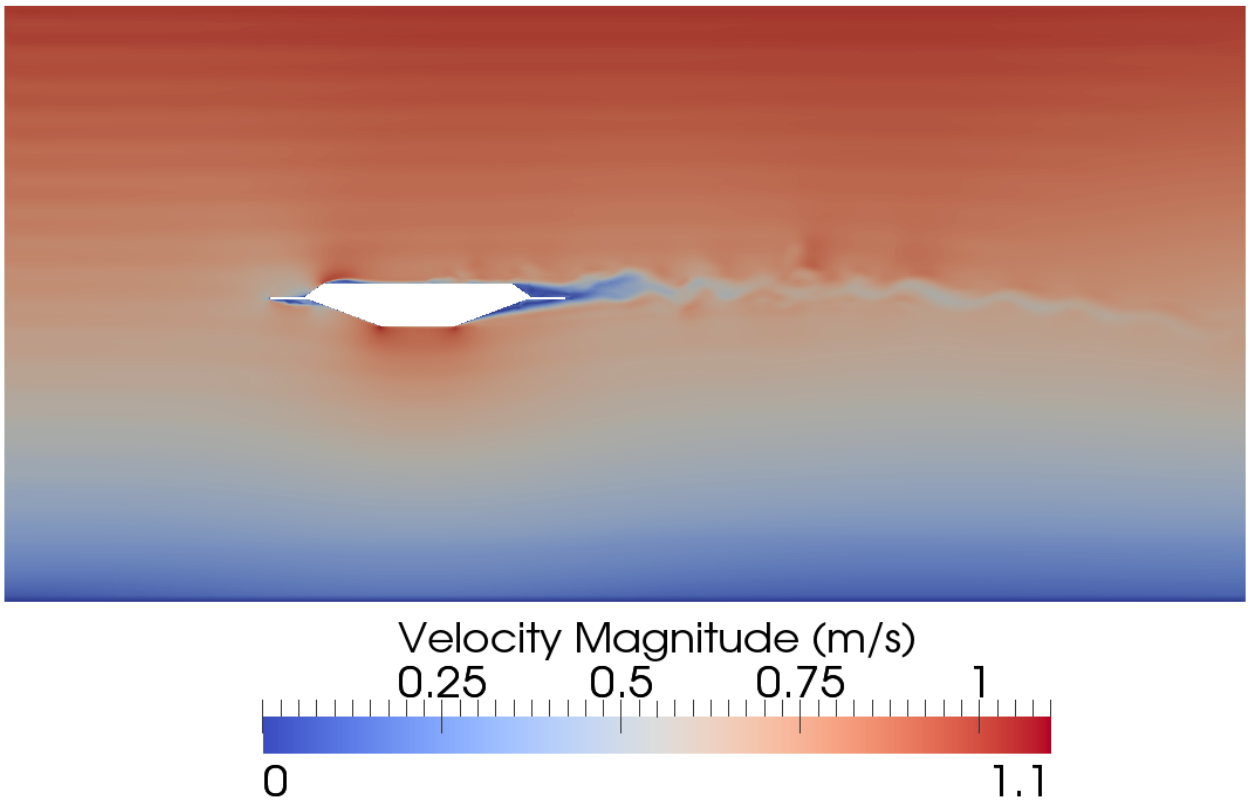

Figure 4-8 - Velocity magnitude contour plot for the Humber Bridge simulation.

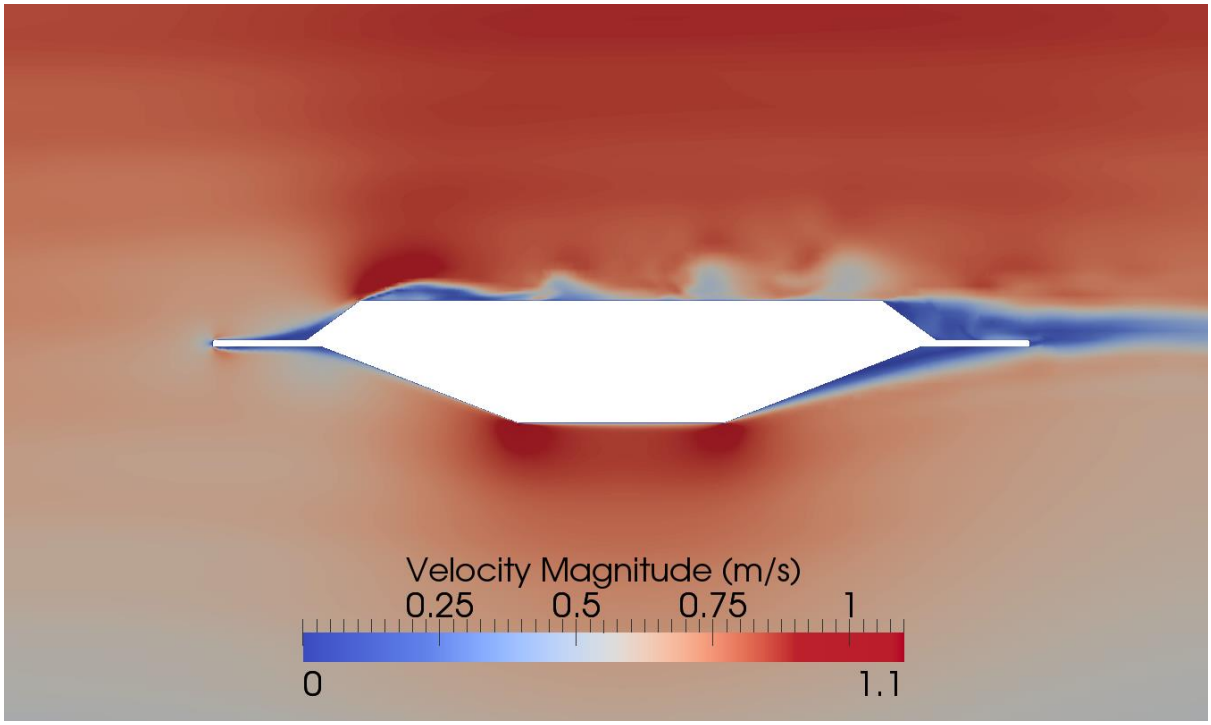

Figure 4-9 - Velocity magnitude contour plot showing three single shear layer vortices being convected along the top wall of the bridge deck.

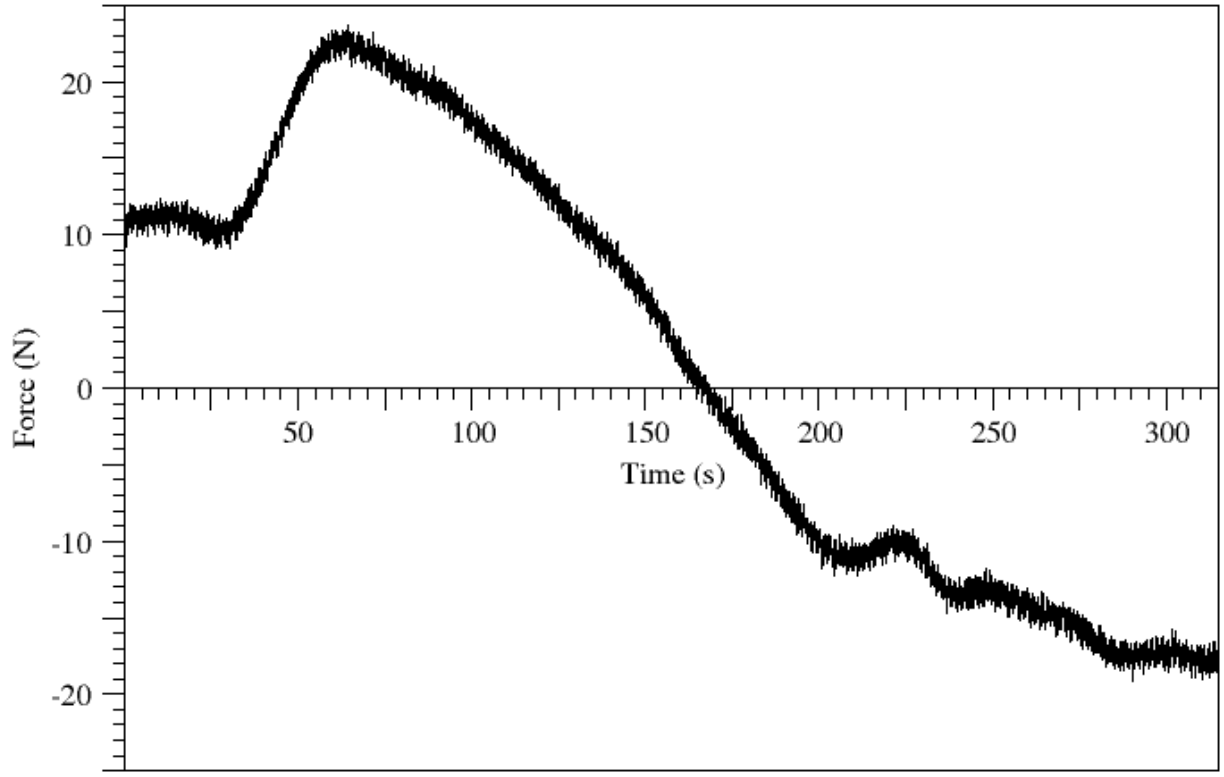

Figure 4-10 – Graph showing the lift force on the Humber Bridge against time.

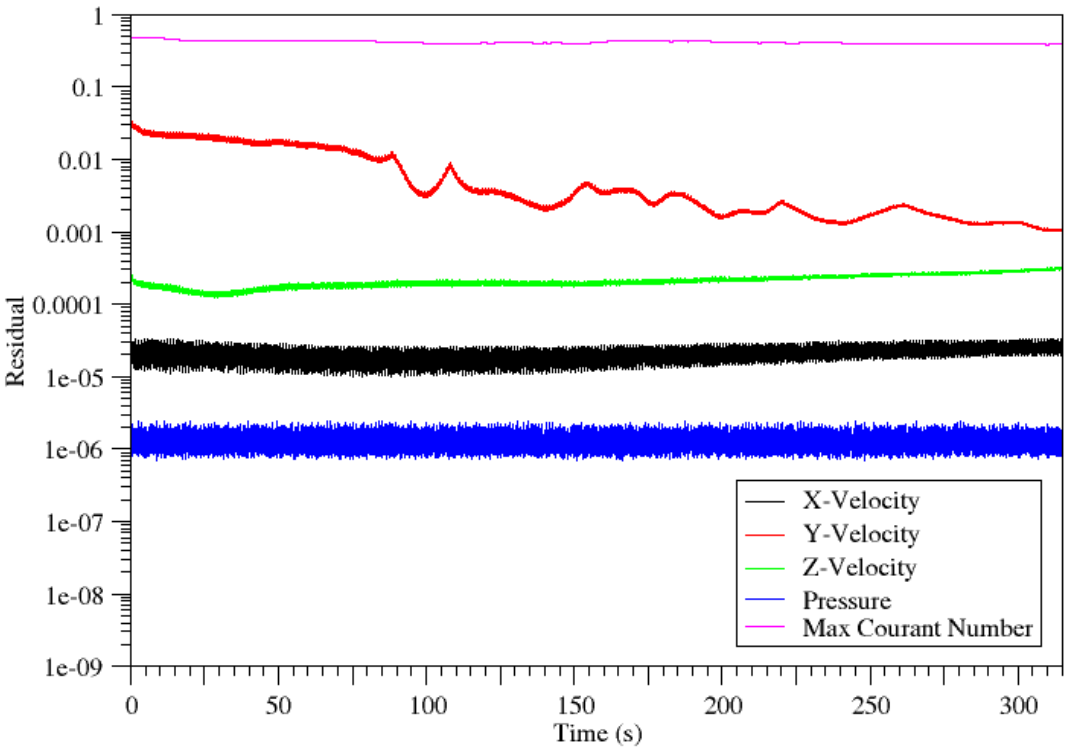

Figure 4-11 Residual plot for the Humber Bridge simulation

4.4. Analysis of Humber Bridge Simulation Results

Unlike the square cylinder simulations, *Figure 4-8* does not show a clear indication of alternating, asymmetrical, vortex shedding; suggesting that the Von Kármán vortex street has been supressed. The suppression of the Von Kármán vortex street is related to the geometry of the bridge. As was discussed in the literature review, physical barriers which are placed in the stagnation region of a bluff body, can cause a large reduction in the frequency and strength of vortex shedding. The Humber Bridge cross section shows a typical trapezoidal box girder geometry with the addition of large fins on either side of the deck. These fins were designed to reduce vortex induced vibrations [39]. The fins streamline the bluff body, preventing separation. As a result vortex shedding is reduced.

A closer inspection of the contour plot in
Figure 4-8 shows that there is a slight indication of a periodic motion in the wake of the bridge. As there is no Von Kárman vortex street, there must be another form of vortex formation which is causing the periodic motion. *Figure 4-9* shows a close up of the bridge deck, 30 seconds before the image shown in *Figure 4-8*. In this image we can see three single shear layer vortices which have formed at the leading edge of the horizontal section of the deck. These vortices are convected along the surface of deck until they reach the wake. These vortices are different to

the single shear layer vortices discussed in the literature review. These vortices are not a result of heaving, nor do they travel at 60% of the bulk velocity (they travel at 100%). Regardless, these single shear vortices are likely to be responsible for the periodic motions of the wake

Figure 4-10 shows the Z component of force which the fluid imparts on to the bridge. The most notable thing about this graph is the unusual step rise of the graph at the beginning, followed by the gradual decent into the negative region of the graph. Looking at literature, the Humber bridge was designed so that it would have a negative coefficient of lift [39]. As such we would expect that the force on the bridge would always be in the negative region of the graph. These results suggest that the simulation has not reached a steady state until roughly 250 seconds, where the graph starts to converge. Examination of a small region of the force graph shows that there is a consistent oscillating pattern throughout the simulation. With the aid of V. Triay Jiménez, Fourier transform analysis has been carried out on the data and has been provided to the structural sub group for comparison purposes. This graph can be viewed in *Figure 4-12*.

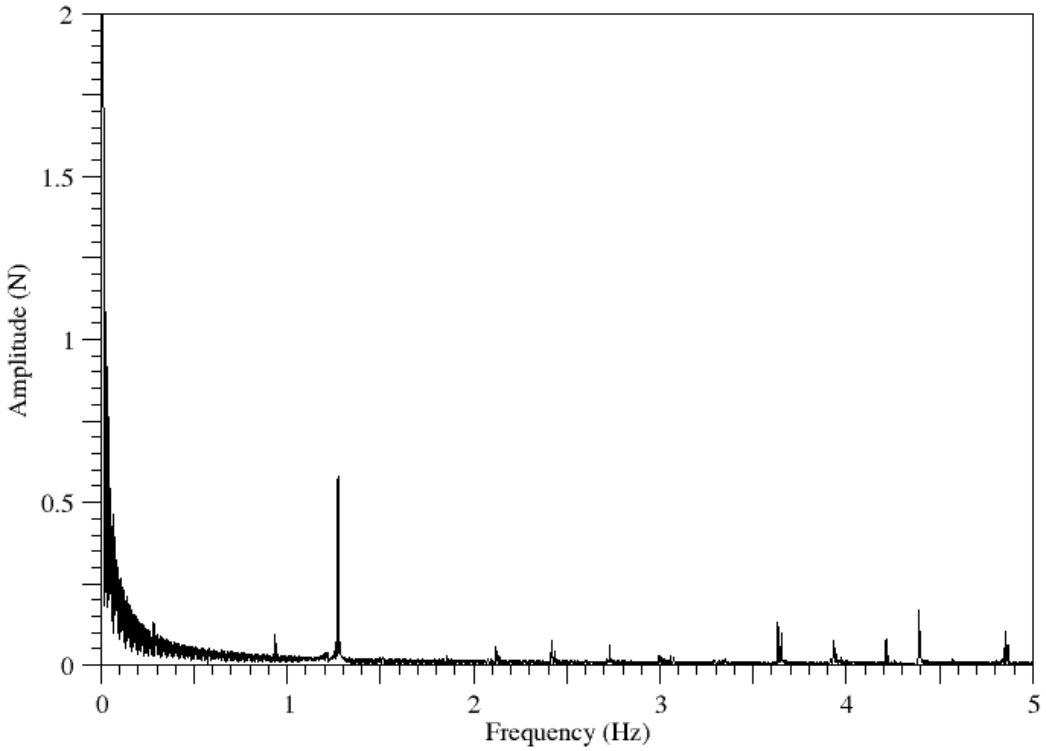

Figure 4-12 - Fast Fourier tranform analysis of the graph shown in Figure 4-10

The residual plot shown in *Figure 4-11* shows good results. The pressure residual consistently remained at $1x10^{-6}$. The velocity residuals are low and also show stability and convergence. Finally the maximum Courant number in the simulation stayed below 1 for the entire simulation, averaging just under a value of 0.4.

Whilst mesh refinement was carried out, the y^+ values are not quite low enough. *Figure 4-13* shows the y^+ values of the cells next to the bridge. Whilst some cells did reach the desired criteria, the majority fall in the range of 10 – 30, with the cells at the corners of the deck showing y^+ values as high as 80. As with the square cylinder case, this is likely to cause inaccuracies in the results. To correct this would require further mesh refinement. Unfortunately simulations are limited by the computational power available. This simulation ran for over two weeks. Carrying out further mesh refinement will lead to unreasonably long computational times. The first solution to this problem is to spend large sums of money on more powerful computers. The second solution is to restructure the mesh.

The original plan was to create a mesh similar to the mesh in *Figure 3-3* (A). Whilst extensive attempts were made, snappyHexMesh did not perform as expected. To create the desired mesh a different meshing program will have to be used. As none of the CFD subgroup members had much experience with other mesh generation software, this was not possible at the time. However if a different software can be mastered, then some of the unnecessary refinement in the X and Y directions can be removed, and the mesh can be refined further in the Z axis. The effect of the high y^+ values on this simulation is currently unknown. Based on the square cylinder case (where similar y^+ values were achieved) an inaccuracy in the shedding frequency of 15% might be expected.

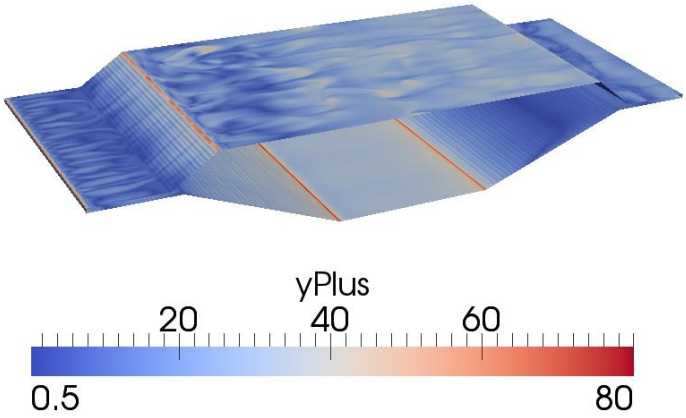

Figure 4-13 - Image showing the y^+ values for the cells next to the bridge deck.

4.5. Simulation Assumptions

As with most CFD simulations, assumptions have been made which may lead to slight inaccuracies in the results. The first assumption is similar to an assumption highlighted in the literature review. The simulations presented here have just investigated a plain bridge deck. The barriers, cars, bridge cables, and other obstructions have not been simulated here. As was

shown in research, the addition of barriers to a bridge simulation can introduce vortex shedding where previously there was none [20]. This could mean that frequencies not predicted in these simulations could be present on the actual bridge. Further assumptions have been made with the geometry of the plain deck. Creating a mesh is easier if a geometry has straight edges which meet at sharp corners. As a result, some of the curved edges and finer details of the deck have been omitted. The effect of these omissions is unknown.

One assumption which is likely to have a large impact on the results, is (at the moment) unavoidable. The simulation presented here assumes that the deck cannot move. If the deck is stationary then some forms of vortex shedding (such as low speed vortex excitations) cannot be predicted. Furthermore, whilst the movement of air has an effect on the bridge, the movement of the bridge also has an effect on the air. This can have unpredicted effects in the forms of unusual vortex shedding mechanisms or amplification of existing vortices [15]. The solution to this problem would be to use a dynamic mesh. A dynamic mesh allows a structure to move, usually by squashing or stretching the surrounding cells. The use of a dynamic mesh will drastically increase the cost of simulation. The simulation has already taken 2 weeks to run. It already requires a finer mesh, and as it has only just reached convergence ideally it would be run for a longer time (possibly until 400 seconds). Consequently, the use of a dynamic mesh here would lead to an impractically long simulation run time.

5. Discussion and conclusions

The initial aims of this project were threefold; to investigate the interactions of fluid with static objects, to investigate the different ways of modelling turbulence, and to create an accurate representation of fluid moving past the Humber Bridge. The first aim was completed through an investigation into vortex shedding mechanisms. The most common vortex shedding mechanism was deemed to be the Von Kármán vortex street, and is characterised by asymmetrical, alternating, vortex shedding in the wake of bluff bodies. This mechanism was classed as a two shear layer mechanism. Other two shear mechanisms exist, such as symmetrical vortex shedding, which occurs in low speed fluctuating flows. Single shear vortex shedding mechanisms are also achievable. One type of single shear flow was investigated; it formed in the wake of a bluff body placed under a heaving motion.

In addition to these investigations, methods of suppressing vortex shedding were briefly looked at. The stagnation region of flow was found to be a large influence on the strength and formation of vortices. The addition of physical objects, such as splitter plates in the stagnation region, were shown to supress common vortex mechanisms such as the Von Kármán vortex street. Other suppression methods were also investigated. The cross sectional geometry of trapezoidal box girder decks was shown to affect the generation of vortices. Additional work was suggested in this field.

The second aim was completed through an investigation into different types of LES modelling. The original Smagorinsky-Lilly model was found to have inaccuracies due to a variance in C_{SGS}. This issue was overcome with a slight change to the model, forming the dynamic SGS model. The SGS stresses in this model were related to the local rate of strain of the resolved eddies, rather than the strain of the entire flow. A need for accurate modelling of vibrations at high Reynolds numbers spurred the creation of DES; a hybrid model of RANS and LES. This model is successful in situations where a specific type of mesh has been used. Nevertheless, some situations require the use of an ambiguous mesh (*Figure 3-3* (B)). This can lead to inaccuracies in DES results. This issue was overcome with the development of DDES, a model which detects the boundary layer of a problem before activating the switching function. DDES was predicted to become the standard formulation of DES.

LES simulations of a square cylinder case were carried out. In these simulations Von Kármán vortex streets were successfully simulated. Unfortunately the y^+ values of the cells next to the wall were too high. This is thought to be most probable cause of the inaccurate vortex shedding frequency that resulted. Afterward, completion of the third and final aim was attempted.

A section of the Humber Bridge deck was modelled and meshed. Due to the type of mesh created, DDES was chosen as the most appropriate turbulence model. The air was set to travel at $1ms^{-1}$ across the deck. 315 seconds of air flow was simulated, taking 2 weeks and 2 days to complete. The results of the simulation do not show a Von Kármán vortex street. This is thought to be a design feature of the bridge. The vortex suppression has been linked to the added fins on the sides of the bridge. There was evidence of a periodic motion in the wake of the bridge. This is a result of the formation of single shear layer vortices at the leading edge of the bridge. These vortices are convected along the bridges body until they reach the trailing edge

whereupon they coalesce with the wake. This vortex formation was shown to produce a periodic force on the bridge.

A graph of force against time was created for the simulation. The graph showed that for the first 175 seconds there was a positive lift force acting on the bridge. The bridge was designed to have a negative lift coefficient meaning that during the first 175 seconds the simulation had not reached a steady state. At approximately 250 seconds the graph did converge to a negative value. Fourier transfer analysis was carried out on the last 65 seconds of the simulation, these results were provided to the structural sub group for comparison purposes.

As with the square cylinder case, the y^+ values in the Humber bridge simulation were too large. Unfortunately this project is limited by the computing power available. Whilst mesh refinement is required, the refined mesh would create an unreasonably long simulation. The suggested solution to this issue is to restructure the mesh, so that the cells next to the boundary are wide but thin, as shown in *Figure 3-3* (A). The current mesh has an unnecessary amount of refinement in the X and Y directions. The restructure would hopefully decrease the y^+ values, without increasing the number of cells.

5.1. Further Work

The first suggestion for further work would be to test different wind speeds. In this project only one wind speed was tested ($1ms^{-1}$). Ideally multiple wind speeds would have been tested. Carrying out multiple simulations would allow any trends between wind speed and vortex shedding frequency to be identified. Unfortunately the long simulation run time prevented further investigations from being carried out. The reason that $1ms^{-1}$ was chosen for this project was because it is a low velocity. As velocity increases, the time step that is used must decrease in order to keep the courant number below 1. The relationship between velocity and required time step is a linear one. It should be clear to the reader that simulating high wind speeds can also lead to unreasonable simulation run times.

Another consideration with regards to the setup of the simulation is changing the angle of attack of the wind. In this simulation the net movement of air was only in the X direction. In real life the wind can approach from any direction. The angle of attack is likely to affect the vortex shedding in different ways, either affecting the strength, frequency, or type of shedding

produced. Consequently, all angles of attack must be investigated before one can definitively say that a particular wind speed will not cause the bridge to vibrate at one of its modes.

5.2. Closing Remarks

The main aim of the CFD subgroup was to create an accurate representation of turbulence passing over a bridge. The simulations carried out here show positive results; single shear layer vortices were shown to form at the leading edge and were convected along the bridge to the trailing edge, the vortex suppressing fins successfully prevented a Von Kármán vortex street from forming, the simulation showed that the bridge has a negative lift coefficient (albeit took 250 seconds to reach this point), and finally, the frequencies of the wind induced vibrations were obtained from the simulations. Whilst there were inaccuracies, the solutions to these issues all require more computational power; something which is currently unavailable.

Due to the nature of the CFD program that was used, now that the simulation has been set up, very little user input is required to change a modelling parameter. Changing the wind speed or angle of attack requires changing a few numbers in various directories. Of course the simulation will have to be run again for at least two weeks, but once running, the simulations require minimal human supervision or input.

When attempting a project such as this one there is a choice to make. The project can be completed using wind tunnel simulations or CFD simulations. Wind tunnel simulations are very fast. A wide range of velocities and a wide range of angles of attack can be completed in a single day. Data collected from these simulations are on par (and sometimes better) than the information that can be gained from CFD. Wind tunnel testing does come with the large drawback of cost. Wind tunnel tests can easily cost tens of thousands of pounds, depending on the size of the wind tunnel and amount of time needed.

CFD simulations are comparatively very cheap. Whilst the initial cost of buying a cluster is large, running costs are equivalent to the price of electricity and wages for the CFD user. Once setup, CFD simulations can easily be tweaked or changed with little user input. As highlighted in this report, the simulations can take a very long time to complete. As was demonstrated here, one angle of attack at a low speed took over two weeks. Ultimately it is up to the user to determine which approach is the best; however with computational power increasing, CFD is becoming a faster, more viable option for users.

6. Sustainability, Health and Safety, and Project management

6.1. Sustainability

The only impact that this project had on the environment was in the form of energy consumption; from the continual use of a computer. The average desktop computer uses at most 250 watts of power, this translates to 96kWh for a 2 week simulation [40]. The computers used in this project will likely have a slightly higher power consumption than the average desktop, but it will be in this region. The alternative, wind tunnel testing, uses huge amounts of energy. The 10ft x 10ft wind tunnel that NASA owns uses between 20,000 -200,000 kW of electricity per hour [41]. As wind tunnel tests can run for hours at a time, CFD is the obvious choice for environmentally friendly work.

6.2. Health and Safety

The majority of time spent on this project, was carried out sitting at a desk, using a computer. The risks and mitigation strategies associated with this work are summarised in *Table 6.1*.

Table 6.1 - Risk assessment of prolonged work at a workstation. The information which is summarised here can be found in detail in [42].

Risk	Effect of the Risk	Cause of the Risk	Risk Mitigation Strategy
Static loading on the musculoskeletal system	Fatigue and discomfort	Poor Seating posture	• Good lumbar support • No excess pressure on the underside of thighs and backs of knees • Foot support if necessary • Plenty of leg room to allow for postural changes • Arms are horizontal • Wrists are not excessively bent
Prevention of full lung expansion	Difficulties breathing normally		
Slouching or slumping	Vertebrae being pulled out of alignment		
Eye Strain	• Sore, tired, burning or itchy eyes • Difficulty focusing on objects • Double vision • Headaches • Increased sensitivity to light	Prolonged exposure to bright light (caused by glare or staring at a bright screen)	• Reposition the computer screen to avoid glare • Use blinds to avoid glare • Place the screen at a comfortable viewing distance • Ensure the screen is kept clean • Ensure that the room is well lit • Take regular breaks away from the computer

6.3. Project Management

Unlike other types of work, in a CFD project an increase in user input will not speed up the completion of a CFD simulation. Consequently careful planning was required to ensure that simulations were completed on time without failures. Advice from the group's supervisor, Dr Gavin Tabor, gave clear indication that the final simulation (the DDES simulation of the Humber Bridge) would take in the region of several weeks to complete. As such an assessment of the risk of project failure was created to aid with time management.

Risk	Likelihood /10	Severity /10	Importance L*S	How risk was mitigated
Unable to find data for Humber Bridge geometry	2	4	8	Contact was made with Prof. James Brownjohn who has carried out research on the Humber Bridge. He provided technical drawings of the bridge.
Unable to create a suitable mesh for the problem	5	6	30	The meshing program was used multiple times for other simulations before attempting the final simulation
LES is improperly set up	3	8	24	LES models were run on short simulations so that common pitfalls were learnt and avoided.
Humber Bridge simulation crash	2	10	20	The simulation was started early to allow for issues. Simulation choices were made which prioritised stability over speed (discretisation schemes, no. of pressure iterations, etc.). A turbulent inlet condition was used, this can aid with LES stability.
Humber bridge simulation taking longer than expected.	5	4	20	The simulation was started early to allow for any problems. A low wind speed was chosen for the case study.

The Gant chart used to plan this project can be found in *Table 6.2*

Table 6.2 Gant chart used for planning in this individual project.

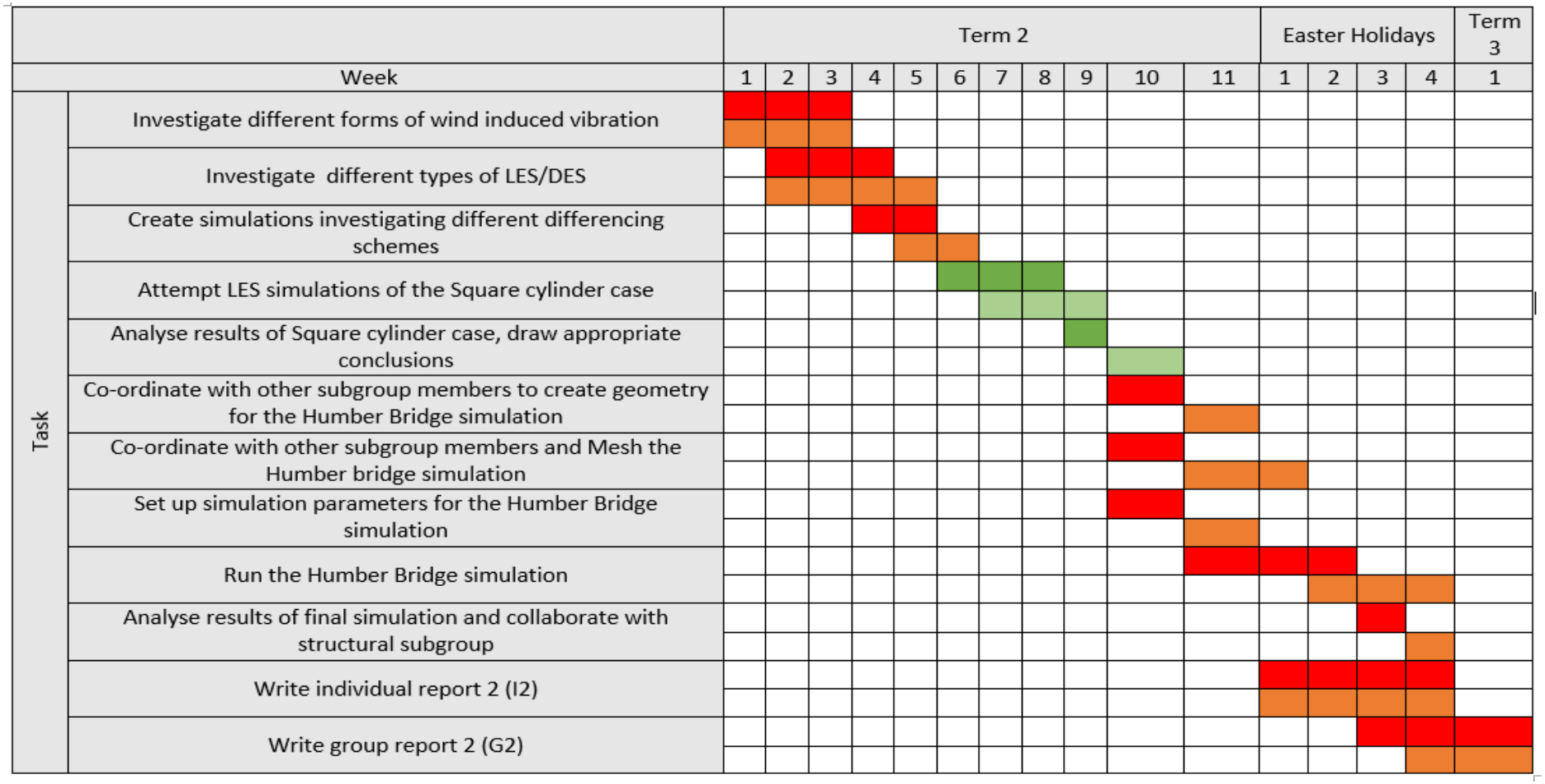

In addition to the aforementioned risk assessment and Gant chart, weekly meetings were attended to improve collaboration between subgroups, and a personal log book was kept for project notes.

7. Contribution to group functioning

The group was split into two subgroups; the structural subgroup and the CFD subgroup. As one of three members of the CFD subgroup, there were large amounts of teamwork, particularly at the start of the project. The CFD in this project was carried out on a program called OpenFOAM. All three members of the subgroup were new to OpenFOAM at the start of the year. During the process of learning how to use OpenFOAM a reciprocal pupil-teacher relationship developed in the team as each subgroup member learnt a different aspect of the program. J. Richmond was the first team member to use the blockMesh feature, and successfully taught the rest of the group how to use it. J. Mullins spent large amounts of time using snappyHexMesh and was happy to give tips and advice in the meshing of a domain. The author of this report spent time investigating discretisation schemes and meshing requirements for different turbulence models. As such he was able to give advice to group members in these matters.

Later in the project, during the creation of the Humber Bridge simulation, there were once again large amounts of teamwork between the subgroup. Each member aided in the creation of various parts of the simulation; J. Richmond created the inlet boundary conditions, J. Mullins created the geometry and started the meshing, whilst the author of this report set up initial conditions, boundary conditions, discretisation schemes and made appropriate turbulence modelling choices. As was indicated, there was problems meshing the geometry. At one point all three members of the subgroup were working on the Humber Bridge mesh. All three members were tweaking parameters and exploring advice found on forums relating to the meshing problem. During this period communication with each other was vital; letting other subgroup members know what forum threads were useful and what advice was not.

At the very end of the group project there was co-operation between the two subgroups. Having successfully modelled the Humber Bridge data extraction and processing was required. The author of this report liaised with D. Fieldhouse and P. Lambton to determine what data was

required from the simulation. After extracting and partially processing the data, fast Fourier transformation of a force – time graph was required. The author, having very little experience with Matlab, enlisted the help of V. Triay Jiménez who, after her project, was more familiar with the software. After resolving some initial hurdles the Fourier transfer was completed and provided to D. Fieldhouse and P. Lambton.

During the course of the project, the author found that there were huge amounts of collaboration and crossover in the CFD subgroup. Unfortunately, due to the nature of the project, there was little teamwork between the two subgroups until the very end of the project. Formal weekly group meetings allowed group members to stay updated on each other's progress, but the author believes that a few small changes will improve teamwork hugely. For any future teams that are attempting a similar project, the author recommends having regular informal meetings, or at least have all members of the project working in the same room. The good cohesion between the CFD subgroup can be attributed to ability to quickly share problems, and discuss possible solutions on a day to day basis. From an overview of the two subgroups, it may seem that problems are unlikely to overlap but, this may not be the case. J. Richmonds experience with coding and understanding of C++ might have been of great use to V. Triay Jiménez in her Matlab based project. D. Fieldhouse has a good understanding of meshing using ANSYS Workbench; the meshing problems experienced by the CFD subgroup may have been quickly resolved with an approach using this program. These suggestions have been made in the hope that future groups can learn from this authors experiences and potentially improve on the success of this project.

8. References

[1] Fujino, Y., & Siringoringo, D. (2013). Vibration mechanisms and controls of long-span bridges: A Review. *Structural Engineering International*, *23*(3), pg. 248-268

[2] Billah, K.; R. Scanlan (1991). "Resonance, Tacoma Narrows Bridge Failure, and Undergraduate Physics Textbooks" *American Journal of Physics 59 (2)*: pg. 118–124.

[3] Strogatz, Steven et al. (2005). "Theoretical mechanics: Crowd synchrony on the Millennium Bridge," *Nature, Vol. 438*, pg. 43-44.

[4] Richmond, J. (2015) Inlet conditions for simulating turbulent atmospheric air flow, *Exeter University, ECMM102, I2 report.*

[5] Mullins, J. (2015) Topographical and environmental effects on fluid flow using computational techniques, *Exeter University, ECMM102, I2 report.*

[6] Morgan, J. (2014), Modelling of Turbulent Effects on a Bridge Deck Structure Using Computational Methods, *Exeter University, ECMM102, I1 report.*

[7] Bull, M. K., & Luxton, R. E. (1991). Vortex-shedding and the maintenance of thick turbulent boundary layers on long cylinders in axial flow. In *Advances in Turbulence 3* (pp. 13-21). Springer Berlin Heidelberg.

[8] Sakamoto, H., & Haniu, H. (1990). A study on vortex shedding from spheres in a uniform flow. *Journal of Fluids Engineering*, *112*(4), 386-392.

[9] Von Kármán, T. (1963) Aerodynamics. McGraw-Hill, ISBN 978-0-07-067-602-2, pg. 69-71

[10] Von Karman, T. (1911). Über den Mechanismus des Widerstandes, den ein bewegter Körper in einer Flüssigkeit erfährt. Nachrichten von der Gesellschaft der Wissenschaften zu Göttingen, *Mathematisch-Physikalische Klasse*, *1911*, 509-517.

[11] Cahalan, B (1999) Landsat 7 Reveals Large-scale Fractal Motion of Clouds, NASA, *retrieved from: http://earthobservatory.nasa.gov/IOTD/view.php?id=625 on: 03/12/2014*

[12] Toet, W. (1999) Surface Finishes – Why are they not used on an F1 car. *Retrieved from: http://www.formula1-dictionary.net/dimpled_surface_finish.html on: 21/04/2015*

[13] Pankanin, G. L. (2007, May). Experimental and Theoretical Investigations Concerning the Influence of Stagnation Region on Karman Vortex Shedding. In *Instrumentation and Measurement Technology Conference Proceedings, 2007. IMTC 2007. IEEE* (pp. 1-6).

[14] Kumar, P. P. (2009). The effect of Von Kármán vortex street on building ventilation. In *Proceedings of the World Congress on Engineering* (Vol. 2).

[15] Bearman, P. W. (1984). Vortex shedding from oscillating bluff bodies. *Annual Review of Fluid Mechanics*, *16*(1), 195-222.

[16] Nakamura, Y., & Nakashima, M. (1986). Vortex excitation of prisms with elongated rectangular, H and [vertical, dash] cross-sections. *Journal of Fluid Mechanics*, *163*, 149-169.

[17] King, R. (1977). A review of vortex shedding research and its application. *Ocean Engineering*, *4*(3), 141-171.

[18] Shiraishi, N. & Matsumoto, M. (1981) Vortex-induced oscillation of bluff bodies. *Proceedings of JSCE*, pg. 3-12

[19] Matsumoto, M. (1999). Vortex shedding of bluff bodies: a review. *Journal of Fluids and Structures*, *13*(7), 791-811.

[20] Larsen, A., & Wall, A. (2012). Shaping of bridge box girders to avoid vortex shedding response. *Journal of Wind Engineering and Industrial Aerodynamics*,*104*, 159-165.

[21] Smagorinsky, J. (1963). General circulation experiments with the primitive equations: I. the basic experiment. *Monthly weather review*, *91*(3), pg. 99-164.

[22] Deardorff, J. W. (1970). A numerical study of three-dimensional turbulent channel flow at large Reynolds numbers. *Journal of Fluid Mechanics*, *41*(02), pg. 453-480.

[23] Lilly, D. K. (1967). The representation of small scale turbulence in numerical simulation experiments. *National Center For Atmospheric Research*, 281, pg. 195-210

[24] Rogallo, R. S., & Moin, P. (1984). Numerical simulation of turbulent flows.*Annual Review of Fluid Mechanics*, *16*(1), 99-137.

[25] Leslie, D. C., & Quarini, G. L. (1979). The application of turbulence theory to the formulation of subgrid modelling procedures. *Journal of fluid mechanics*, *91*(01), 65-91.

[26] Clark, R. A., Ferziger, J. H., & Reynolds, W. C. (1979). Evaluation of subgrid-scale models using an accurately simulated turbulent flow. *Journal of Fluid Mechanics*, *91*(1), 1-16.

[27] McMillan, 0. J., & Ferziger, J. H. (1979). Direct testing of subgrid-scale models.*AIAA Journal*, *17*(12), 1340-1346.

[28] Bardina, J., Ferziger, J., & Reynolds, W. (1980). Improved subgrid-scale models for large-eddy simulation. *AIAA 13th Fluid & Plasma Dynamics Conference, Snowmass Colorado*

[29] Germano, M., Piomelli, U., Moin, P., & Cabot, W. H. (1991). A dynamic subgrid-scale eddy viscosity model. *Physics of Fluids A: Fluid Dynamics (1989-1993)*,*3*(7), 1760-1765.

[30] Bakker, A. (2006). Applied computational fluid dynamics. *Computational Fluid Dynamic, Engs*, *150*.

[31] Blasius, H. (1908). "Grenzschichten in Flüssigkeiten mit kleiner Reibung". *Z. Math. Phys.* **56**: 1–37.

[32] Spalart, P. R., Jou, W. H., Strelets, M., & Allmaras, S. R. (1997). Comments on the feasibility of LES for wings, and on a hybrid RANS/LES approach. *Advances in DNS/LES*, *1*, 4-8.

[33] Strelets M. (2001). Detached eddy simulation of massively separated flows. *Presented at AIAA Aerosp. Sci. Meet. Exhib., 39th, Reno, Pap. No. AIAA-2001-0879*

[34] Spalart, P. R., Deck, S., Shur, M. L., Squires, K. D., Strelets, M. K., & Travin, A. (2006). A new version of detached-eddy simulation, resistant to ambiguous grid densities. *Theoretical and computational fluid dynamics*, *20*(3), 181-195.

[35] Spalart, P. R. (2009). Detached-eddy simulation. *Annual Review of Fluid Mechanics*, *41*, 181-202.

[36] Germano, M., Piomelli, U., Moin, P., & Cabot, W. H. (1991). A dynamic subgrid-scale eddy viscosity model. *Physics of Fluids A: Fluid Dynamics (1989-1993)*,*3*(7), 1760-1765.

[37] Lyn, D. A., & Rodi, W. (1994). The flapping shear layer formed by flow separation from the forward corner of a square cylinder. *Journal of fluid Mechanics*, *267*, 353-376.

[38] Lyn, D. A., Einav, S., Rodi, W., & Park, J. H. (1995). A laser-Doppler velocimetry study of ensemble-averaged characteristics of the turbulent near wake of a square cylinder. *Journal of Fluid Mechanics*, *304*, 285-319.

[39] Walshe, D. E., & Cowdrey, C. F. (1972). A further aerodynamic investigation for the proposed Humber Suspension Bridge. *Transport and Road Research Laboratory* (No. R&D Rept).

[40] Bluejay, M., (2014) How much electricity do computers use? *Retrieved from: http://michaelbluejay.com/electricity/computers.html on: 27/04/15*

[41] NASA Glenn Research Centre (2009) Glenn Research Centre Fact Sheet – Flying on the Ground, r*etrieved from: http://www.nasa.gov/centers/glenn/about/fs05grc.html on: 27/04/15*

[42] Health and Safety Executive (2002) Work with display screen equipment, *retrieved from: http://www.hseni.gov.uk/l26_work_with_display_screen_equipment.pdf* on: 27/04/15